

# Diverging network architecture of the *C. elegans* connectome and signaling network

**Sophie Dvali<sup>1</sup>, Caio Seguin<sup>2,3</sup>, Richard Betzel<sup>4,5</sup>, and Andrew M. Leifer<sup>1,6\*</sup>**

<sup>1</sup>Princeton University, Department of Physics, Princeton, NJ, United States of America

<sup>2</sup>University of Melbourne and Melbourne Health, Melbourne Neuropsychiatry Centre, Melbourne, Victoria, Australia

<sup>3</sup>Indiana University, Department of Psychological and Brain Sciences, Bloomington, IN, USA

<sup>4</sup>University of Minnesota, Department of Neuroscience, Minneapolis, MN, USA

<sup>4</sup>Masonic Institute for the Developing Brain, Department of Neuroscience, Minneapolis, MN, USA

<sup>6</sup>Princeton University, Princeton Neurosciences Institute, Princeton, NJ, United States of America

\*leifer@princeton.edu

**ABSTRACT**

The connectome describes the complete set of synaptic contacts through which neurons communicate. While the architecture of the *C. elegans* connectome has been extensively characterized, much less is known about the organization of causal signaling networks arising from functional interactions between neurons. Understanding how effective communication pathways relate to or diverge from the underlying structure is a central question in neuroscience. Here, we analyze the modular architecture of the *C. elegans* signal propagation network, measured via calcium imaging and optogenetics, and compare it to the underlying anatomical wiring measured by electron microscopy. Compared to the connectome, we find that signaling modules are not aligned with the modular boundaries of the anatomical network, highlighting an instance where function deviates from structure. An exception to this is the pharynx which is delineated into a separate community in both anatomy and signaling. We analyze the cellular compositions of the signaling architecture and find that its modules are enriched for specific cell types and functions, suggesting that the network modules are neurobiologically relevant. Lastly, we identify a "rich club" of hub neurons in the signaling network. The membership of the signaling rich club differs from the rich club detected in the anatomical network, challenging the view that structural hubs occupy positions of influence in functional (signaling) networks. Our results provide new insight into the interplay between brain structure, in the form of a complete synaptic-level connectome, and brain function, in the form of a system-wide causal signal propagation atlas.

## Introduction

How the structure of a biological system supports its functional repertoire is a central question in biology. A defining feature of this question is that it seeks to relate two lenses into the same biological system. In neuroscience, the relevant structural lens is the network map of synaptic connections in the brain, called a “connectome”, which is typically measured using electron microscopy and captures the wiring of the nervous system. The functional lens is given by network maps that report how the activity of one neuron in the brain either relates to or influences the activity of others. These can be measured by functional MRI, electrophysiology, or calcium imaging. Network science provides a powerful toolkit to characterize and distill key properties of these networks [1, 2]. There has been an implicit hypothesis that since network properties capture fundamental features of the brain they should persist across both of these lenses. However, in studies in humans, there is evidence that network properties can differ, sometimes dramatically, between function and structure, including measures of centrality [3, 4] and community structure [5, 6, 7]. Therefore, the extent to which properties of a brain’s structural network match properties of its functional network remains unclear, especially at brain scale and cellular level.

With few exceptions [8, 9, 10], the link between the synapse level wiring of a brain’s connectome and its function has not been explored in detail and at scale, and the mapping between the two may not be trivial. One reason that structure and function may differ is that some wired connections may exist without a corresponding functional connection. Gene expression or neuromodulators may transiently activate subsets of connections from a menu of all possibilities [11, 12]. Similarly, there is evidence of functional connections that exist in the absence of wiring. Some of these can be attributed to extrasynaptic signaling, where one neuron releases peptides or other transmitters via dense core vesicles that diffuse through the extracellular milieu to activate other neurons [13, 14, 15, 16, 17, 18, 19, 20]. Other functional connections that lack direct wiring can arise from multi-step pathways—so-called “poly-synaptic paths”, where one neuron signals to another, which in turn signals to another [21, 22]. All of these effects make it challenging to translate between the networks of structure and function.

Until now, it has been difficult to empirically compare brain structure and function, as this requires both synapse-level maps of anatomical wiring as well as corresponding causal maps of how one neuron’s

activity influences another's. Recently, we measured a brain-wide causal “Signal Propagation Atlas” of the nematode *C. elegans* via direct optogenetic activation and simultaneous whole-brain calcium imaging [14]. This directed network describes the flow of signals between 23,433 pairs of neurons in response to controlled and systematic stimulation of individual neurons. Its connections, therefore, represent the “effective” connection between pairs of neurons, taking into account mono- and poly-synaptic signaling pathways, and extrasynaptic signaling. Uniquely and in contrast to previous correlation-based measures of functional connectivity, this dataset provides causal information about signaling between neurons. Critically, this signaling network is accompanied by a complete connectome of chemical synapses and gap junctions between pairs of neurons [23, 24, 25] allowing us to directly compare the physical wiring of a nervous system with the causal signal flow at scales ranging from an individual synapse to the entire brain.

Here, we investigate and compare the properties of both networks: wiring and signaling, focusing on their community structure and rich club. We show that along these dimensions, and with only a few notable exceptions, properties of the signaling network differ from the underlying connectome. We focus further on the hierarchical community structure of the signaling network and show that, despite exhibiting only a weak correspondence with connectome communities, its communities are significantly enriched for specific cell classes and functions. One area of agreement is the community of pharyngeal neurons, which is defined similarly in both networks, but which interacts with the rest of the network differently. Finally, we compare the rich clubs of both networks and find only minimal overlap in terms of membership. Collectively, our findings suggest that the effective signaling network, which measures the collective influence of direct, indirect, and extrasynaptic signaling pathways, has different network properties from the underlying connectome.

## Results

Here, we compare the network properties of the *C. elegans* connectome [23, 24, 25] –the network of chemical and electrical synapses of the brain– to a recently-constructed network map of neural signaling [14] of the genetically identical brain. While the connectome encodes only direct synaptic connections between neurons, the signaling network captures effective connections that arise from the combined effect of not only direct connections but also all interactions that span multiple hops through the anatomical

network (poly-synaptic chains), as well as extrasynaptic signaling that is not constrained to flow along synapses. We consider binarized directed connectome and signaling networks of the same head neurons ( $N = 188$  head neurons from a total of 302 neurons in the entire nervous system) but each having different numbers of edges (corresponding to  $M = 1151$  for signaling and  $M = 3250$  for the connectome). Thus, the networks differ in terms of their density ( $d_s = 0.033$  and  $d_a = 0.092$ ) and their distribution of motifs (Supplementary Fig. 2). The signaling network has an average clustering coefficient of 0.13, a bit less than half of the anatomical network's clustering coefficient of 0.3. The *C. elegans* connectome is well known to be a small world network [26, 27]. Similarly, we find that the signaling network is also small world ( $\sigma_s = 4.76$  and  $\sigma_a = 2.52$  for the signaling and anatomical head networks, respectively).

### **Hierarchical community structure differs between signal propagation and anatomy**

We chose to compare the complex architecture of wiring and signaling networks by means of their hierarchical modular structure. Neural networks are hierarchically divided into sub-networks, referred to as modules, communities, or clusters [28, 29, 30, 31, 32, 33]. This modular composition is thought to shape neural communication, by providing a balance between segregation into specialized functional units and integration of information across distant neural elements [7] and therefore informs how the nervous system performs computations [34, 35, 36]. In fMRI studies, abnormalities in modular structure serve as biomarkers of neuropsychiatric conditions [37]. Modular structure has been used to interpret both anatomical [38, 39, 7] and functional [5, 40] representations of neural networks. Yet, it remains unclear whether modular structure should be conserved in these different views, and in some cases evidence suggests they are not [6, 41].

We explicitly tested whether the anatomical and signaling descriptions of the *C. elegans* brain shared a similar modular structure. We used a hierarchical variant of the stochastic block model (SBM) to independently subdivide the wiring and signaling networks into nested communities [42, 43, 44, 45, 46]. We found stark differences in the modular organization of these two views into the *C. elegans* brain. The anatomical connectome was clustered into 20 communities in the first hierarchical level, with the smallest containing only one neuron and the largest containing 20 (Fig. 1 b, anatomical clusters are denoted by Arabic numerals). In contrast, the signal propagation network was optimally partitioned

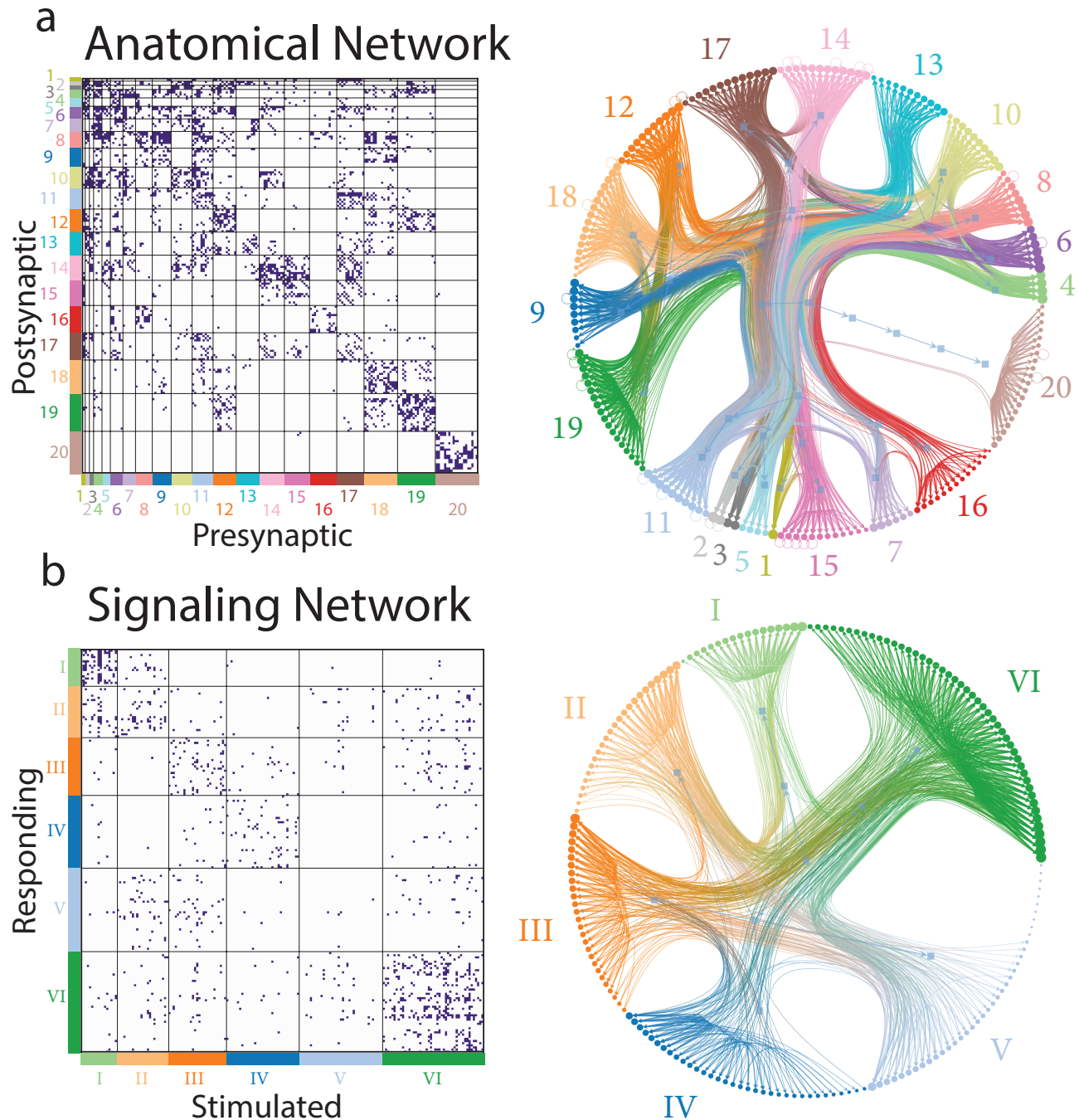


**Figure 1. Hierarchical modular structure of the *C. elegans* signal propagation and anatomical networks.** a) Left: matrix showing anatomical connectivity. Each pixel indicates the presence or absence of synaptic contacts from one individual neuron in the brain to another, from [23, 24, 25]. Neurons are sorted by community assignment of the first hierarchical level, the smallest community first, and then subsequent communities increasing in size. Right panel: circular dendrogram showing community assignments at different hierarchical levels, colored corresponding to the first level. b) Left panel: signal propagation network matrix. Each pixel indicates whether a downstream neuron exhibits robust calcium activity in response to an upstream neuron's optogenetic stimulation [14]. Organized similarly to (a). Right panel: same as in (a) for the signal propagation network.

Community I	I2L, I2R, I3, I4, IL2R, M1, M2L, M2R, M3L, M3R, M4, MCL, MCR, MI, NSML, NSMR, URYVR
Community II	AVL, BAGL, BAGR, CEPVL, I1L, I1R, I6, IL1DL, IL1DR, IL1VL, IL1VR, IL2DR, IL2VR, M5, OLLL, OLLR, OLQDR, OLQVR, RIPR, RMER, SAADL, URBR, URYDL, URYVL
Community III	AFDL, AIML, AIMR, AIYL, AIYR, ASJL, AUAL, AUAR, AVBL, RICL, RIH, RIML, RIMR, RMDDR, RMDL, RMFL, RMFR, RMGL, SABVL, SABVR, SIBVR, SMBDL, SMBVL, SMBVR, SMDDL, SMDDR, VB2
Community IV	ADAL, ADAR, ADEL, ADER, AIBR, AINL, AIZL, AIZR, AQR, AS1, AVFL, AVFR, AVG, AVKL, AVKR, DB1, DB2, DD1, FLPL, FLPR, RIBL, RIBR, RICR, RIFR, RIGL, RIGR, RIS, RMHL, SABD, SIBVL, SMBDR, URBL, VA1, VB1
Community V	ADFR, AIAL, AIAR, AIBL, ALA, AWCL, CEPVR, DA1, I5, IL1L, IL1R, IL2DL, IL2L, IL2VL, OLQDL, OLQVL, RID, RIFL, RIPL, RIR, RMDDL, RMED, RMEL, RMEV, RMGR, SAADR, SIADL, SIADR, SIAVL, SIAVR, SIBDL, SIBDR, URADL, URADR, URAVL, URAVR, URYDR, VD1, VD2
Community VI	ADFL, ADLL, ADLR, AFDL, AINR, ASEL, ASER, ASGL, ASGR, ASHL, ASHR, ASIL, ASIR, ASJR, ASKL, ASKR, AVAL, AVAR, AVBR, AVDL, AVDR, AVEL, AVER, AVHL, AVHR, AVJL, AVJR, AWAL, AWAR, AWBL, AWBR, AWCR, CEPDL, CEPDR, RIAL, RIAR, RIVL, RIVR, RMDR, RMDVL, RMDVR, SAAVL, SAAVR, SMDVL, SMDVR, URXL, URXR

**Table 1. Community assignments of the signaling network (first hierarchical level).**

into six communities in the first hierarchical level, the smallest of which contained 17 neurons and the largest of which contained 47 neurons (Fig. 1 a, signal propagation clusters are denoted by Roman numerals). Interestingly, the signaling network exhibited fewer hierarchical levels compared to the anatomical network (three levels composed of six, three, and one communities for the signaling network, and five levels composed of twenty, eight, three, two, and one communities for the connectome).

Next, we investigated the distribution of bilateral pairs across communities. A majority of *C. elegans* neurons consist of bilaterally symmetric pairs that are often connected to each other via gap junctions and tend to have similar gene expression [15], wiring [23], and correlated activity patterns [9]. As we would expect, bilaterally symmetric neurons are much more likely to be found in the same communities than across different communities, for both the anatomical and signaling networks. In the anatomical network, bilateral neuron pairs were 38 times more likely to be in the same community than in different communities ( $p = 1.5 \times 10^{-210}$ ) and in the signaling network, they were twice as likely ( $p = 4 \times 10^{-45}$ ). This finding is consistent with the hypothesis that some features should be conserved across both network

Community 1	RIH
Community 2	RIBL, RIBR
Community 3	RIAL, RIAR
Community 4	AIBL, AIBR, RIML, RIMR
Community 5	URYDL, URYDR, URYVL, URYVR
Community 6	AVEL, AVER, RIGL, RIGR, RIS, RMFL
Community 7	AVKL, AVKR, SAADL, SAADR, SAAVL, SAAVR
Community 8	AVAL, AVAR, AVBL, AVBR, AVDL, AVDR, AVL, RID
Community 9	ADAL, ADAR, ALA, AQR, AVG, AVJL, AVJR, FLPL, FLPR
Community 10	RIVL, RIVR, RMDL, RMDR, RMFR, SIAVR, SMDDL, SMDDR, SMDVL, SMDVR
Community 11	ADEL, ADER, RICL, RICR, RMGL, RMGR, URBL, URBR, URXL, URXR
Community 12	ADFL, ADFR, AIZL, AIZR, AUAL, AUAR, AWBL, AWBR, BAGL, BAGR, RIR
Community 13	SIADL, SIADR, SIAVL, SIBDL, SIBDR, SIBVL, SIBVR, SMBDL, SMBDR, SMBVL, SMBVR
Community 14	IL1L, IL1R, OLLL, OLLR, RMDDL, RMDDR, RMDVL, RMDVR, RMED, RMEL, RMER, RMEV
Community 15	IL1DL, IL1DR, IL1VL, IL1VR, IL2VL, IL2VR, RIPL, RIPR, URADL, URADR, URAVL, URAVR
Community 16	AS1, DA1, DB1, DB2, DD1, SABD, SABVL, SABVR, VA1, VB1, VB2, VD1, VD2
Community 17	CEPDL, CEPDR, CEPVL, CEPVR, IL2DL, IL2DR, IL2L, IL2R, OLQDL, OLQDR, OLQVL, OLQVR, RMHL
Community 18	ADLL, ADLR, AIML, AIMR, ASHL, ASHR, ASJL, ASJR, ASKL, ASKR, AVFL, AVFR, AVHL, AVHR, RIFL, RIFR
Community 19	AFDL, AFDR, AIAL, AIAR, AINL, AINR, AIYL, AIYR, ASEL, ASER, ASGL, ASGR, ASIL, ASIR, AWAL, AWAR, AWCL, AWCR
Community 20	I1L, I1R, I2L, I2R, I3, I4, I5, I6, M1, M2L, M2R, M3L, M3R, M4, M5, MCL, MCR, MI, NSML, NSMR

**Table 2. Community assignments of the anatomical connectome (first hierarchical level).**



descriptions.

## **Anatomical and signal propagation communities have mostly non-overlapping membership**

If the community architecture of the signaling and anatomical networks is similar we would expect signal propagation communities to either correspond to specific partners in the anatomical network, or since there are fewer signaling communities, we would expect some signaling communities to entirely contain anatomical communities. To test whether signaling and anatomical communities follow this straightforward correspondence, we first calculated the pairwise overlap between each of the signal propagation and anatomical communities (Fig. 2 a). With only one exception (community **I**), signal propagation communities did not neatly map onto or wholly contain anatomical communities. Most signal propagation communities had neuron membership that was spread across multiple anatomical communities (rows of Fig. 2 a). Similarly, all anatomical communities had neuron membership that was spread across many signal propagation communities (columns of Fig. 2 a). These findings suggest that most signal propagation communities are not trivially mapped onto nor trivially contain anatomical communities.

Even without a trivial mapping between signal propagation and anatomical communities, we nonetheless sought to identify the “best-matched” signal-anatomy community pairs. We therefore calculated the extent to which each signal propagation community was enriched for anatomical communities, and compared this to a null hypothesis in which neurons are assigned to communities at random [47], (Fig. 2 b). Clustering was performed on this enrichment map to assign best-matched pairs (Fig. 2 c), as described in the methods. The majority of signaling communities (four of six) were statistically significantly enriched for at least one anatomical community. However, to be a relatively strong match, we would expect a signaling community to have statistically significant enrichment for only one community. We find only two of the signaling communities had statistically significant enrichment for exactly one of the anatomical communities. This suggests that the majority of signaling communities (four of six) had only weak pairing to their best-matched anatomical pair.

Across all analyses, the pairing of signaling community **I** and anatomical community **20** stands out as an exception. These two communities neatly correspond to one another– 93% of signaling community **I**'s

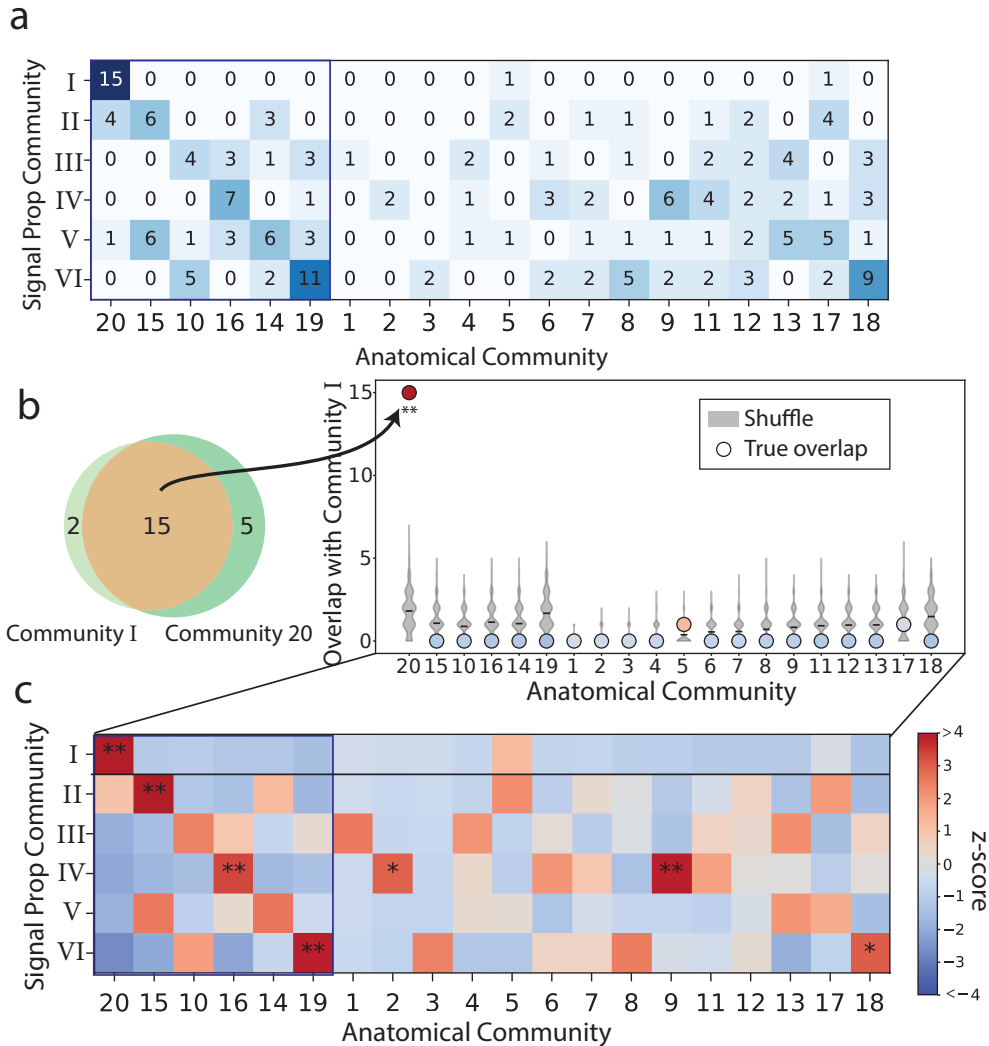


**Figure 2. Comparison between anatomical and signal propagation communities. a)** Overlap (counts) between membership of anatomical and signal propagation communities is shown. Community best-matching is performed via a similarity matrix and the Hungarian method, as described in the methods. **b)** Left: Venn diagram illustrating the true overlap (intersection) between the set of neurons in signaling community I and the set of neurons in the anatomical community 20. Right: Community I's number of overlapping neurons for each anatomical module (circles). Relative enrichment (circle color) is calculated as a z-score of the true overlap compared to a null distribution of shuffled community assignments (grey violin plots), described in methods. Circle color corresponds to color bar in c. **c)** Relative enrichment of overlap is reported as a z-score for each anatomy-signaling community pair (\*  $p < 0.05$ , \*\*  $p < 0.01$ , p-values from same distribution as z-score, FDR-adjusted).

neurons are members of anatomical community **20**, while 75% of anatomical community **20**'s neurons are members of signaling community **I**. Similarly, both communities are statistically significantly enriched only for one another.

Why might communities **I** and **20** neatly correspond, when others do not? These two communities are comprised almost exclusively of pharyngeal neurons (Fig. 3 c,d). The pharynx has long been hypothesized to be largely functionally autonomous [48, 49], partly because it makes only two extrapharyngeal synaptic connections to the rest of the network (Fig. 1 a) [23, 24, 25]. Its role in controlling pharyngeal pumping and feeding behaviors has historically been assumed to operate largely independently of the rest of the network [49, 48]. This stark anatomical isolation may explain why both the structural and signaling networks preserve this community organization. It is interesting that, even with this direct correspondence between the anatomical and signaling communities of the pharyngeal neurons, in the signaling network, the community of pharyngeal neurons is much more highly connected to the other communities than it is in the anatomical network (Fig. 1 a), highlighting differences between the brain's wiring and signaling.

Collectively, our results suggest that, in general, modular structure is not conserved across anatomical and functional descriptions of the brain. In the discussion, we speculate that a combination of polysynaptic signaling, extrasynaptic signaling, and non-functional anatomical wiring may contribute to these differences. The pharynx is an exception and suggests that in cases where a sub-network of neurons is extremely isolated in the anatomical network, its modularity may be preserved even in the functional description. However, even here, it is notable that the patterns of connectivity between the modules still differ.

### **Communities are enriched for neuron type and role**

Clustering of anatomical networks has previously been used to identify communities of neurons that are enriched for cell types or known functional cellular roles, including in *Drosophila* and *C. elegans* [50, 51, 52, 53, 54, 55]. Consistent with prior findings, our modular clustering of the *C. elegans* anatomical network recapitulates anatomical communities that are each significantly enriched for no more than one of the three *C. elegans* neuron cell types classes: Sensory, Inter- and Motor neurons [27](Fig. 3 c; Supplementary Fig. 4 a; Table 2). Similarly, they are each enriched for no more than one of five predefined cell roles (pharyngeal, amphid sensory, locomotory inter-, vnc motor and ring interneurons) (Fig. 3 d;

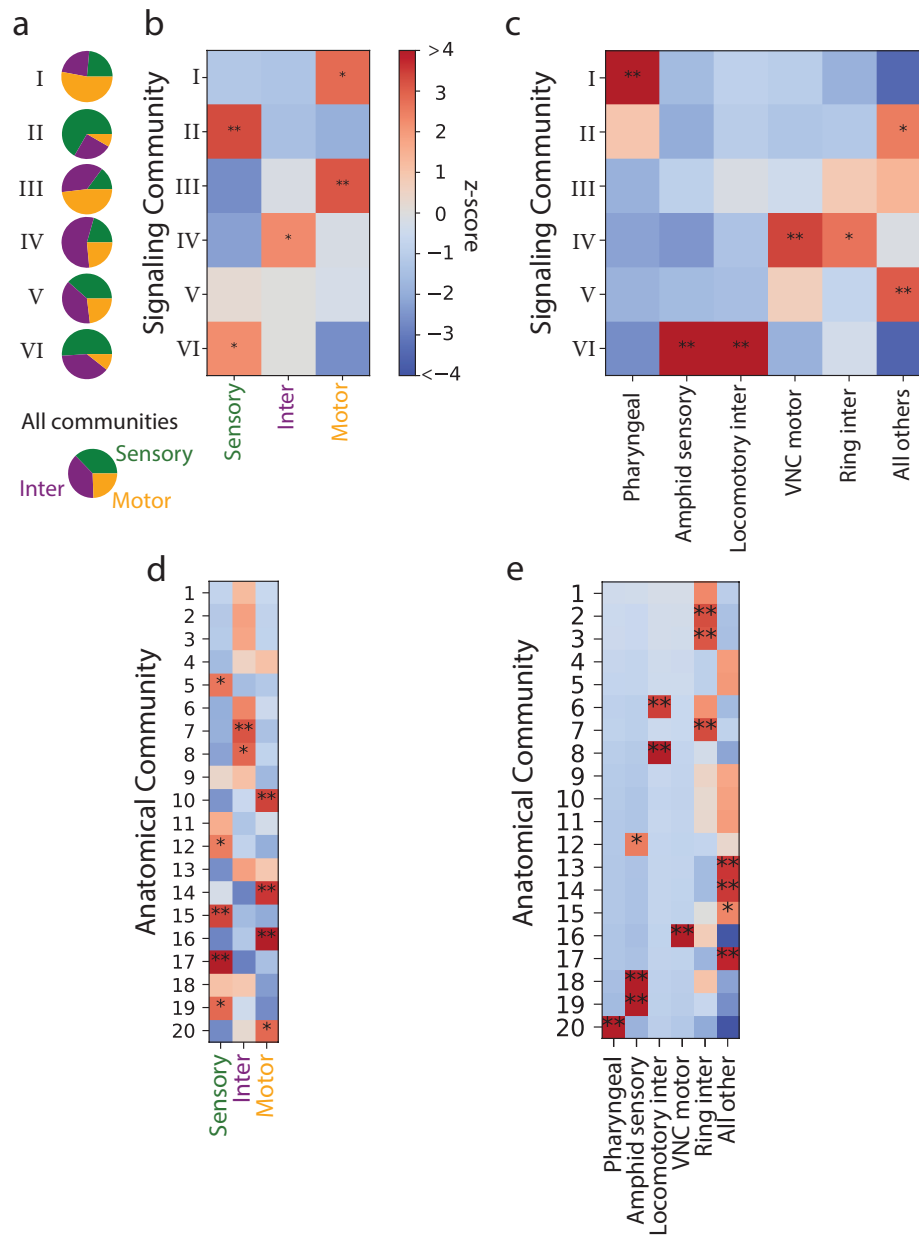


**Figure 3. Communities are enriched for neuron type and role.** **a**) Fractional breakdown of signaling community neuron membership into sensory, inter-, and motor neurons cell type (green, purple, and yellow respectively). **b**) Enrichment (z-score) of signaling communities for sensory, inter-, and motor neurons (\*  $p < 0.05$ , \*\*  $p < 0.01$ , p-values FDR-adjusted) **c**) Enrichment of signaling communities for neuron role (\*  $p < 0.05$ , \*\*  $p < 0.01$ , p-values FDR-adjusted) **d**) Enrichment (z-score) of anatomical communities for sensory, inter-, and motor neurons (\*  $p < 0.05$ , \*\*  $p < 0.01$ , p-values FDR-adjusted), **e**) Enrichment of anatomical communities for neuron role (\*  $p < 0.05$ , \*\*  $p < 0.01$ , p-values FDR-adjusted)

Supplementary Fig. 4 b; Table 2). Enrichment is calculated by comparison to a null hypothesis of randomly shuffled assignments as described in methods. We next explored cell-type annotation in the signaling network.

Signaling network communities, like the anatomical communities, also showed clear enrichment for distinct cell types. Each signaling community was statistically significantly enriched for no more than one of three previously defined cell type classes (Fig. 3 a,b; Supplementary Fig. 4 a; Table 1). Only one of the six communities, **V**, showed no significant enrichment for any cell type.

Similarly, cell roles are well segregated into different signaling communities. As mentioned in the previous section community **I** contains almost all the pharyngeal neurons. All but one locomotory interneuron are members of community **VI** (Fig. 3 c; Supplementary Fig. 4 b; Table 1). Along with interneurons involved in locomotion, community **VI** was also enriched for the amphid sensory neurons. The amphid sensory neurons are the primary olfactosensory neurons of *C. elegans* and play a role in chemotaxis and mechanosensation [56, 57, 58]. The locomotor interneurons AVA, AVD, and AVE from this community, among others, translate this sensory signal into behavior to control and initiate backward locomotion [59, 60, 61, 62, 63]. Similarly, neuron AVB from this community is a key part of the forward locomotory circuit [64]. The community structure may therefore have defined a cluster in such a way as to capture a sensorimotor pathway.

Community **IV**, the only community that was enriched for interneurons, was not only specifically enriched for ring interneurons but also for VNC motor neurons. The neurons that make up the ring interneurons have been less well characterized than the locomotor interneurons but are thought to integrate sensory signals and information about the inner state of the organism to drive behavioral decisions likely through VNC motor neurons which innervate dorsal and ventral muscles to induce locomotion [65, 23, 66].

That signaling communities are enriched for cell type, and that cell roles are segregated into different communities, sometimes in sensible ways, suggests that our signaling measurements reflect known functional roles in the brain and also provides evidence that the stochastic block model analysis extracts meaningfully defined communities.

## **Anatomy is net feed-forward along the sensorimotor path while signaling is ambiguous**

It is commonly expected that there should be overall feed-forward signaling from sensory neurons to interneurons to motor neurons [27]. Anatomically, synaptic edges are enriched in a feed-forward manner from sensory neurons to interneurons to motor neurons (Supplementary Fig. 5 b,c). By contrast, the signaling network is not appreciably feed-forward along this path compared to a shuffle control (Supplementary Fig. 5 b,c). This is also visible in the connectivity between and among communities. We do not see any obvious evidence of feed-forwardness when looking at how communities that are enriched for sensory, inter, and motor neurons signal to each other (Supplementary Fig. 6).

## **Linking neurobiological annotations to community motifs**

To gain insight into large-scale network organization, we identified stereotyped inter-community relations, called “community motifs” that assign a label to how each community interacts with each other community, either assortative, disassortative, or core-periphery (Fig. 4 a) [67]. Different community interactions provide hypotheses about the roles that communities may play when interacting. For example, the presence of assortative communities, which are internally dense but externally sparse, can be evidence of separate computational units. We observe, as expected, that the majority of community interactions in both signal propagation and anatomical networks are assortative (70% for both networks) [67, 50, 68]. In both networks, neurons most frequently participated in assortative interactions Fig. 4 b).

We were particularly interested in investigating core-periphery interactions because they can be evidence of broadcasting and integrating information. Core-periphery interactions are comprised of one densely connected core of “driver” nodes with substantial connections to a periphery that, in turn, is sparsely connected internally. We observed that in the anatomical network, 26% and in the signaling network, 30% of community interactions are core-periphery and we wondered which types of neurons may be involved in this broadcasting and integrating motif.

Strikingly pharyngeal and amphid sensory neurons were significantly enriched for participation in the “core” component of the core-periphery interactions in the signal propagation network (Fig. 4 d). However, in the anatomical network, these same neurons were impoverished for their coreness and instead were significantly enriched for participation in the assortative community motif. We assessed the enrichment

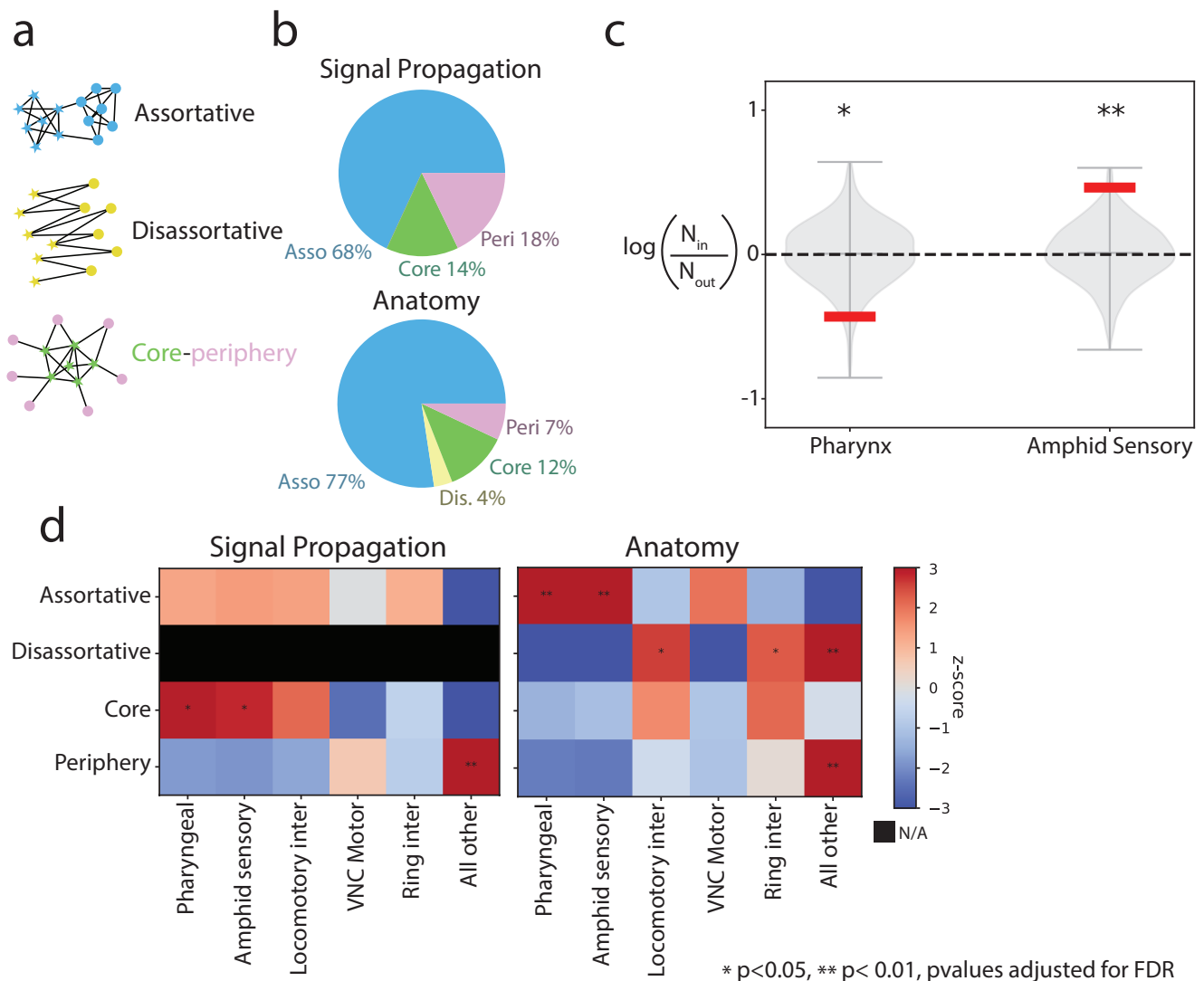


**Figure 4. The Pharynx and Sensory neurons make up the core of "core-periphery" interactions. a)** Example schematic of Assortative, Disassortative, and Core-periphery community interactions **b)** Pie charts of the average fraction of participation of each node in the different community interactions for the signal propagation network (Top Panel) and the anatomical network (Bottom Panel). **c)** Log of the ratio of incoming and outgoing connection to the pharynx and the amphid sensory neurons (red bar) compared to null distribution from networks where the neuron role assignments have been shuffled (grey violin plot) (\* p<0.05, \*\* p<0.01). **d)** Enrichment (z-score) of neurons of different roles for participation in assortative, disassortative, and core/periphery interactions in the signaling network (Left Panel) and anatomical network (Right Panel). Signaling network has no disassortative interactions. (\* p<0.05, \*\* p<0.01, p-values FDR-adjusted)

of neurons for participation in these different interaction types, by calculating a z-score comparing the actual interactions participated in to those obtained from randomly shuffled community interactions. These results show that the divergence between anatomical and signaling modules goes beyond a mere reassignment of nodes into communities, but rather indicates the presence of a differing architecture in the signaling network which may support modes of neural computation and communication that are not evident from examining only the anatomical architecture.

As participation in the core of a core-periphery interaction could potentially indicate a role for broadcasting or integrating signals, we were curious if the pharyngeal and amphid neurons fit one of these two roles. By inspecting the number of ingoing and outgoing edges in the signaling network, we find that pharyngeal neurons show more broadcasting-like behavior perhaps suggesting a role of sending pumping or food-related signals broadly to the rest of the nervous system (Fig. 4 c). Counterintuitively amphid sensory neurons have more incoming than outgoing edges in the signaling network, possibly suggesting that more research is needed to explore whether they could be serving as integrators (Fig. 4 c). The ratios of incoming to outgoing edges could not trivially be explained by the number of times in which amphid or pharyngeal neurons were observed or stimulated (Supplemental Fig. 8 a,b,c,d).

This change in participation in interaction styles of the same group of neurons between the two networks was also observed in other cell roles, including locomotory interneurons which are enriched for participation in disassortative interactions in anatomy, a motif that signifies a capacity for transmitting signals across the boundaries of communities and which is entirely absent from the signaling network. This switch in interaction styles for the different neuron types between the anatomical network and the signaling network suggests that signaling may be performing neural processing in ways different from what we may expect from looking solely at the anatomical network topology.

### **Anatomy and signaling exhibit rich clubs of mostly non-overlapping neurons**

Like other complex networks [69, 70], the *C. elegans* connectome exhibits “rich-club” connectivity [71], in which highly connected hub nodes are also densely connected to each other. We wondered whether we should also expect to see rich-club features in the signaling network.

We found statistical evidence supporting the hypothesis that the signaling network also displays the



defining feature of rich-club behavior: neurons with a degree of  $k$  or higher highly connected to other neurons of degree  $k$  or higher (Fig. 5 a). The signaling network exhibited a “dual rich club” with two clear tiers: the first tier contained 16 neurons of degree 25 or higher, whereas the second and more exclusive tier contained five neurons of degree 40 or higher (Fig. 5 a,b).

Surprisingly, the sets of neurons that comprised the rich clubs in the signaling network were nearly disjoint when compared to the rich club in the anatomical network (Fig. 5 b,c). Neurons that exhibited the highest degree in the anatomical network tended to have lower degrees in the signaling network (Pearson correlation  $r = 0.22$ ) (Fig. 5 b red shading) while neurons with the greatest degree in the signaling network were less well-connected in the anatomical network (Fig. 5 b blue and green shading). The only exceptions were the two neurons present in both rich-clubs: command interneurons AVEL and AVER. That this bilateral pair of neurons is highly connected in both networks is consistent with its prominent role in the locomotory circuit driving backwards locomotion [59, 61, 60, 63].

We next asked: how are the signaling network’s rich-club neurons distributed across its communities? Do they span multiple communities, linking them to one another, or do they predominantly congregate in one community? Here we consider both tiers of the rich club together ( $k > 25$ ). Community **VI** was highly enriched for hub neurons, containing 10 out of the 16 hub neurons including AVEL and AVER. Rich club neurons also make up a large fraction of this community, approximately 21%. Given that rich club neurons are, by definition, interconnected, it is then consistent that community **VI** is also the most highly self-interconnected community (Supplementary Fig. 6).

Of the remaining rich club neurons, two were in pharyngeal community **I** (M3L, M3R), and several were in communities **II** (OLLR, OLQDR), **III** (RMDDR) and **V** (RMDDL). Surprisingly, members of the rich club were fairly equally spread among sensory, inter-, and motor neurons (Supplementary Fig. 9 b). This is in contrast to the anatomical network where the rich club is primarily composed of interneurons (Supplementary Fig. 9 c). These observations suggest that some neurons historically classified as sensory or motor based on their anatomical wiring may also serve a functional role similar to what has conventionally been ascribed to interneurons.

Due to their nature as highly interconnected and high-degree neurons, we expected that the rich club neurons might function as a core of “core-periphery” interactions. As predicted, in both the anatomical

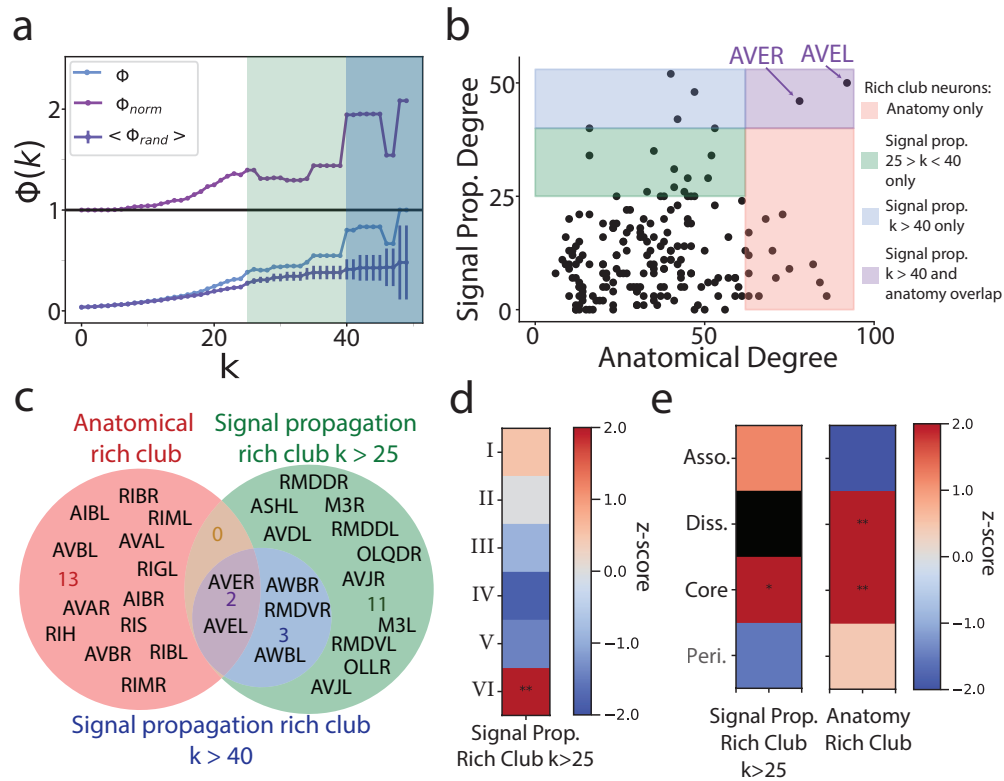


**Figure 5. Rich club of the signaling network.** **a)** Normalised rich club coefficient of the signaling network (purple), rich club coefficients of the empirical signaling network (light blue), and 100 randomized null networks (dark blue; errors bars indicate standard deviation). Rich club regimes are marked by green ( $k > 25$ ) and blue ( $k > 40$ ) shadings. **b)** Signaling degree vs. the anatomical degree of each neuron (Pearson correlation  $r = 0.22$ ). **c)** Venn diagram of the neurons in the anatomical rich club (red), signaling rich club of  $k > 25$  (green) and signaling rich club of  $k > 40$ . **d)** Enrichment (z-score) of the signaling communities for signaling rich club neurons (\*  $p < 0.05$ , \*\*  $p < 0.01$ , p-values FDR-adjusted). **e)** Enrichment (z-score) of neurons belonging to the signaling rich club (left) and the anatomical rich club (right) for assortative, disassortative, and core/periphery interactions in their respective networks.

and signaling networks, each network's respective rich club members were enriched for coreness (Fig. 5 e). The interpretation of the core as integrators/broadcasters of information is well-aligned with the known functions of neurons in the anatomical rich club, like AVA, RIM, and AVB, that coordinate motor responses to sensory signals. It is less obvious how well this description fits those neurons in the signaling rich club, such as AVJ, which have not previously been described as sensory integrators. Our findings suggest that it may be worth further investigation to assess whether these neurons have an additional integration role.

Rich club analysis relies on measures of in- and out-degree. A potential confounding factor is that signal propagation degree is correlated with the number of empirical observations made of each neuron in our experimental dataset (pearsons correlation  $r = 0.71$ , Supplementary Fig. 8 e). We were reassured, however, that rich club members had large degrees well in excess of what we could explain from the correlation (Supplementary Fig. 5 e,f), and not all highly observed neurons are members. Therefore we conclude that membership in the rich club is not a trivial result of being measured often.

## Discussion

Here, we take advantage of a recently compiled signal propagation network in *C. elegans* to investigate how the causal network architecture of the worm compares to its underlying wiring, and ultimately how this maps onto cell type and known neurobiological function. In particular, we test whether features commonly used to characterize networks are preserved across these two network descriptions of the same brain. This is important because, until now, only one network description of a brain has generally been available at a time, and therefore understanding how different network descriptions relate is crucial for extracting insights about neural signaling from a wiring diagram, or vice versa.

As we might expect, there are some similarities between the networks of wiring and signaling. Both are complex networks with hallmark small-world organization, i.e., their wirings are not regular nor random, but poised between these two extremes [26]. The correspondence between the community partitions of the two networks, while small, was still larger than chance, as we expect. Strikingly, both networks had a clear community devoted to the pharynx, consistent with its neurobiological role, as it is thought to be a mostly separate unit of neurons in the *C. elegans* nervous system. This finding suggests that in real-world

brains, it is perhaps only the most extremely pronounced network features, such as the delineation of the nearly isolated pharyngeal sub-network, that are preserved across both signaling and anatomical networks. Even then, we find that in the signaling network the pharynx is less isolated than one would expect from the anatomical network. This could be due, in part, to extrasynaptic signaling from pharyngeal neurons such as M3L which have prominent extrasynaptic connections to other parts of the brain [14].

Other than small-worldness, and the community of pharyngeal neurons, nearly all other aspects of the network were found to be different, including the mapping, delineation, and hierarchy of network modules and the composition of each network's respective rich clubs.

By inspecting the structure of the signaling network, we generate several hypotheses about possible new roles for different classes of neurons.

For example, our analysis finds that the pharynx plays a broadcasting role as the core in “core-periphery” interactions between communities, which suggests that it may send out signals related to pharyngeal pumping and food to the rest of the network. This could help explain how other portions of the brain get access to food intake signals to regulate behaviors such as dwelling [72].

One surprising finding that needs further follow-up is that amphid sensory neurons were found to have more incoming than outgoing edges in the signaling network, suggesting that they may play a potential role as integrators, even though they are primarily known for their role in receiving sensory inputs. Another surprising finding is the diversity of neuron types that are found in the signaling rich club, which span sensory, motor, and interneurons. Together these findings hint at the possibility that the signaling network in *C. elegans* is much more functionally intertwined than previously thought—neurons are listening to more diverse sets of neural inputs and may take on more diverse roles than previously appreciated.

All these differences between the two networks lead us to believe that the signaling network may facilitate types of neural computation and communication that are not obvious when only evaluating the anatomical network and therefore while there is a correspondence between structure and function it is not a direct mapping.

These differences could be due to many factors. It is not always clear which synaptic outputs are functionally relevant and therefore a neuron having many synaptic outputs does not trivially translate to having many functional outputs [14, 8, 10]. Different assumptions about how signals dissipate as

they fan out through the network could also play a role. For example, if a neuron has many anatomical outgoing connections, one could either assume that it has a strong functional impact because it talks to many post-synaptic patterns, or that it has a weak functional impact because its synaptic output is diluted across many paths. In humans, network models that best predict the propagation of focal electrical stimulation take this dilution into account [22] and further work is needed to investigate this in other brains. Additionally, the presence of extrasynaptic signaling invisible to the anatomical network may also explain some of the differences seen in the signaling network [14].

We are reassured to find evidence that the signaling communities are still meaningful, which suggests that the differences may also have meaning. For example, we found that the signaling communities did have alignment to neuron cell roles and class confirming their neurobiological relevance. Most of the communities were enriched for only one of the three neuron classes: sensory, inter-, and motor neurons, as we expected. Additionally, certain communities were enriched for specific neuron functions, as we also expected.

A challenge of any network analysis is that it is subject to the limitations of the experimental measurements used to describe the underlying network. For the signaling network, we are fortunate to be intimately familiar with those limitations. For example, in the calcium imaging experiments used to measure the signaling network, some neurons are observed or stimulated more often than others, and this is quantified [14]. Uneven sampling introduces a bias into which neurons have edges between them. The signal propagation atlas attempts to account for and correct for this bias by only declaring neurons to be functionally connected after employing a statistical framework that explicitly considers both the magnitude of a neurons response as well as the number of observations [14]. Nonetheless, a correlation still persists between the number of times a neuron was observed or stimulated and its in or out degree, respectively, in the signaling network (Supplementary Fig. 8 a, b, e). Here we present evidence to show that this lingering correlation does not solely explain the richness of the members of the anatomical rich club, for example, (Supplementary Fig. 8 e, f) nor can it trivially explain the integrating or broadcasting nature (defined based on the ratio of out to in degree) of the amphid sensory or pharyngeal neurons, respectively (Supplemental Fig. 8 a,b,c,d). In addition, the stochastic block model is implemented in a degree-corrected manner to partition both networks into communities. Future experimental work is needed to more evenly measure

signaling across the network to avoid this confound from the start.

Inhibition is likely systematically undercounted in the underlying measurements of the signaling network due to technical limitations of measuring calcium activity. Because of this, were inhibition to be organized in a systematic way in the network, we would likely not capture that in our analysis. Finally, both of the networks considered here are binarized approximations. We chose a binarized approach because it avoids additional assumptions that would be needed to extract meaningful and comparable weights for both the anatomical and signaling networks, however, future work could explore whether a weighted network approach yields more similarities.

Network neuroscience has made vast strides in identifying topological properties of neural networks with the goal of understanding the brain. It is often implicitly assumed that a brain's network properties such as its partition into modules, its rich clubs, and its small-worldness must be properties of the underlying brain itself, and therefore one would not expect them to depend on the precise lens of network description— whether it is anatomical or signaling. Here we directly compare properties of these two descriptions and find that while some properties are conserved in both the anatomical and signaling networks of the nematode *C. elegans*, many other properties are not. This difference will be important for interpreting network architecture results of newly acquired connectomes [73, 74] and of forthcoming connectomes [75]. We believe efforts to better understand how these different lenses into the brain relate provide an exciting new frontier into network science [76].

## References

1. Bullmore, E. & Sporns, O. Complex brain networks: graph theoretical analysis of structural and functional systems. *Nat. Rev. Neurosci.* **10**, 186–198, DOI: [10.1038/nrn2575](https://doi.org/10.1038/nrn2575) (2009).
2. Bassett, D. S. & Sporns, O. Network neuroscience. *Nat. Neurosci.* **20**, 353–364, DOI: [10.1038/nn.4502](https://doi.org/10.1038/nn.4502) (2017).
3. Power, J. D., Schlaggar, B. L., Lessov-Schlaggar, C. N. & Petersen, S. E. Evidence for hubs in human functional brain networks. *Neuron* **79**, 798–813, DOI: [10.1016/j.neuron.2013.07.035](https://doi.org/10.1016/j.neuron.2013.07.035) (2013).

4. Hagmann, P. *et al.* Mapping the structural core of human cerebral cortex. *PLoS Biol* **6**, e159, DOI: [10.1371/journal.pbio.0060159](https://doi.org/10.1371/journal.pbio.0060159) (2008).
5. Power, J. D. *et al.* Functional network organization of the human brain. *Neuron* **72**, 665–678, DOI: [10.1016/j.neuron.2011.09.006](https://doi.org/10.1016/j.neuron.2011.09.006) (2011).
6. Suárez, L. E., Markello, R. D., Betzel, R. F. & Misic, B. Linking structure and function in macroscale brain networks. *Trends Cogn Sci* **24**, 302–315, DOI: [10.1016/j.tics.2020.01.008](https://doi.org/10.1016/j.tics.2020.01.008) (2020).
7. Sporns, O. & Betzel, R. F. Modular brain networks. *Annu. Rev Psychol* **67**, 613–640, DOI: [10.1146/annurev-psych-122414-033634](https://doi.org/10.1146/annurev-psych-122414-033634) (2016).
8. Creamer, M. S., Leifer, A. M. & Pillow, J. W. Bridging the gap between the connectome and whole-brain activity in *c. elegans*. *bioRxiv* DOI: [10.1101/2024.09.22.614271](https://doi.org/10.1101/2024.09.22.614271) (2024). <https://www.biorxiv.org/content/early/2024/09/23/2024.09.22.614271.full.pdf>.
9. Uzel, K., Kato, S. & Zimmer, M. A set of hub neurons and non-local connectivity features support global brain dynamics in *c. elegans*. *Curr Biol* **32**, 3443–3459, DOI: [10.1016/j.cub.2022.06.039](https://doi.org/10.1016/j.cub.2022.06.039) (2022).
10. Yemini, E. *et al.* Neuropal: A multicolor atlas for whole-brain neuronal identification in *c. elegans*. *Cell* **184**, 272–288, DOI: [10.1016/j.cell.2020.12.012](https://doi.org/10.1016/j.cell.2020.12.012) (2021).
11. Marder, E. Neuromodulation of neuronal circuits: back to the future. *Neuron* **76**, 1–11, DOI: [10.1016/j.neuron.2012.09.010](https://doi.org/10.1016/j.neuron.2012.09.010) (2012).
12. Harris-Warrick, R. M. & Marder, E. Modulation of neural networks for behavior. *Annu. Rev Neurosci* **14**, 39–57, DOI: [10.1146/annurev.ne.14.030191.000351](https://doi.org/10.1146/annurev.ne.14.030191.000351) (1991).
13. Lim, M. A. *et al.* Neuroendocrine modulation sustains the *c. elegans* forward motor state. *Elife* **5**, DOI: [10.7554/eLife.19887](https://doi.org/10.7554/eLife.19887) (2016).
14. Randi, F., Sharma, A. K., Dvali, S. & Leifer, A. M. Neural signal propagation atlas of *caenorhabditis elegans*. *Nature* **623**, 406–414, DOI: [10.1038/s41586-023-06683-4](https://doi.org/10.1038/s41586-023-06683-4) (2023).
15. Taylor, S. R. *et al.* Molecular topography of an entire nervous system. *Cell* **184**, 4329–4347, DOI: [10.1016/j.cell.2021.06.023](https://doi.org/10.1016/j.cell.2021.06.023) (2021).

16. Ripoll-Sánchez, L. *et al.* The neuropeptidergic connectome of *c. elegans*. *Neuron* **111**, 3570–3589, DOI: [10.1016/j.neuron.2023.09.043](https://doi.org/10.1016/j.neuron.2023.09.043) (2023).
17. Beets, I. *et al.* System-wide mapping of peptide-gpcr interactions in *c. elegans*. *Cell Rep* **42**, 113058, DOI: [10.1016/j.celrep.2023.113058](https://doi.org/10.1016/j.celrep.2023.113058) (2023).
18. Smith, S. J. *et al.* Single-cell transcriptomic evidence for dense intracortical neuropeptide networks. *Elife* **8**, DOI: [10.7554/eLife.47889](https://doi.org/10.7554/eLife.47889) (2019).
19. Jékely, G. Global view of the evolution and diversity of metazoan neuropeptide signaling. *Proc Natl Acad Sci U S A* **110**, 8702–8707, DOI: [10.1073/pnas.1221833110](https://doi.org/10.1073/pnas.1221833110) (2013).
20. Thiel, D. *et al.* Large-scale deorphanization of *Nematostella vectensis* neuropeptide g protein-coupled receptors supports the independent expansion of bilaterian and cnidarian peptidergic systems. *eLife* **12**, RP90674, DOI: [10.7554/eLife.90674](https://doi.org/10.7554/eLife.90674) (2024).
21. Seguin, C., Sporns, O. & Zalesky, A. Brain network communication: concepts, models and applications. *Nat. Rev. Neurosci.* **24**, 557–574, DOI: [10.1038/s41583-023-00718-5](https://doi.org/10.1038/s41583-023-00718-5) (2023).
22. Seguin, C. *et al.* Communication dynamics in the human connectome shape the cortex-wide propagation of direct electrical stimulation. *Neuron* **111**, 1391–1401, DOI: [10.1016/j.neuron.2023.01.027](https://doi.org/10.1016/j.neuron.2023.01.027) (2023).
23. White, J. G., Southgate, E., Thomson, J. N. & Brenner, S. The structure of the nervous system of the nematode *Caenorhabditis elegans*. *Philos Trans R Soc Lond B Biol Sci* **314**, 1–340, DOI: [10.1098/rstb.1986.0056](https://doi.org/10.1098/rstb.1986.0056) (1986).
24. Cook, S. J. *et al.* Whole-animal connectomes of both *Caenorhabditis elegans* sexes. *Nature* **571**, 63–71, DOI: [10.1038/s41586-019-1352-7](https://doi.org/10.1038/s41586-019-1352-7) (2019).
25. Witvliet, D. *et al.* Connectomes across development reveal principles of brain maturation. *Nature* **596**, 257–261, DOI: [10.1038/s41586-021-03778-8](https://doi.org/10.1038/s41586-021-03778-8) (2021).
26. Watts, D. J. & Strogatz, S. H. Collective dynamics of ‘small-world’ networks. *Nature* **393**, 440–442, DOI: [10.1038/30918](https://doi.org/10.1038/30918) (1998).



27. Varshney, L. R., Chen, B. L., Paniagua, E., Hall, D. H. & Chklovskii, D. B. Structural properties of the caenorhabditis elegans neuronal network. *PLoS Comput. Biol* **7**, e1001066, DOI: [10.1371/journal.pcbi.1001066](https://doi.org/10.1371/journal.pcbi.1001066) (2011).
28. Betzel, R. F. & Bassett, D. S. Multi-scale brain networks. *Neuroimage* **160**, 73–83, DOI: [10.1016/j.neuroimage.2016.11.006](https://doi.org/10.1016/j.neuroimage.2016.11.006) (2017).
29. Jarrell, T. A. *et al.* The connectome of a decision-making neural network. *Science* **337**, 437–444, DOI: [10.1126/science.1221762](https://doi.org/10.1126/science.1221762) (2012). <https://www.science.org/doi/pdf/10.1126/science.1221762>.
30. Betzel, R. F. Organizing principles of whole-brain functional connectivity in zebrafish larvae. *Netw Neurosci* **4**, 234–256, DOI: [10.1162/netn\[ \]a\[ \]00121](https://doi.org/10.1162/netn[ ]a[ ]00121) (2020).
31. Betzel, R. F., Wood, K. C., Angeloni, C., Neimark Geffen, M. & Bassett, D. S. Stability of spontaneous, correlated activity in mouse auditory cortex. *PLoS Comput. Biol* **15**, e1007360, DOI: [10.1371/journal.pcbi.1007360](https://doi.org/10.1371/journal.pcbi.1007360) (2019).
32. Kiyooka, D. *et al.* Single-cell resolution functional networks during sleep are segregated into spatially intermixed modules. *bioRxiv* DOI: [10.1101/2023.09.14.557838](https://doi.org/10.1101/2023.09.14.557838) (2023). <https://www.biorxiv.org/content/early/2023/09/15/2023.09.14.557838.full.pdf>.
33. Lee, W. A. *et al.* Anatomy and function of an excitatory network in the visual cortex. *Nature* **532**, 370–374, DOI: [10.1038/nature17192](https://doi.org/10.1038/nature17192) (2016).
34. Suárez, L. E., Richards, B. A., Lajoie, G. & Misic, B. Learning function from structure in neuromorphic networks. *Nat. Mach. Intell.* **3**, 771–786, DOI: [10.1038/s42256-021-00376-1](https://doi.org/10.1038/s42256-021-00376-1) (2021).
35. Tanner, J., L., S. M., Coletta, L., Gozzi, A. & Betze, R. F. Functional connectivity modules in recurrent neural networks: function, origin and dynamics (2023).
36. Zhang, R., Pitkow, X. & Angelaki, D. E. Inductive biases of neural network modularity in spatial navigation. *Sci Adv* **10**, eadk1256, DOI: [10.1126/sciadv.adk1256](https://doi.org/10.1126/sciadv.adk1256) (2024).
37. Lynch, C. J. *et al.* Frontostriatal salience network expansion in individuals in depression. *Nature* **633**, 624–633, DOI: [10.1038/s41586-024-07805-2](https://doi.org/10.1038/s41586-024-07805-2) (2024).

38. Sporns, O. Structure and function of complex brain networks. *Dialogues Clin Neurosci* **15**, 247–262, DOI: [10.31887/DCNS.2013.15.3/osporns](https://doi.org/10.31887/DCNS.2013.15.3/osporns) (2013).
39. Sporns, O., Tononi, G. & Kötter, R. The human connectome: A structural description of the human brain. *PLoS Comput. Biol* **1**, e42, DOI: [10.1371/journal.pcbi.0010042](https://doi.org/10.1371/journal.pcbi.0010042) (2005).
40. Bassett, D. S. *et al.* Dynamic reconfiguration of human brain networks during learning. *Proc Natl Acad Sci U S A* **108**, 7641–7646, DOI: [10.1073/pnas.1018985108](https://doi.org/10.1073/pnas.1018985108) (2011).
41. Betzel, R. F. *et al.* Multi-scale community organization of the human structural connectome and its relationship with resting-state functional connectivity. *Netw. Sci.* **1**, 353–373, DOI: [DOI:10.1017/nws.2013.19](https://doi.org/10.1017/nws.2013.19) (2013).
42. Peixoto, T. P. The graph-tool python library. *figshare* DOI: [10.6084/m9.figshare.1164194](https://doi.org/10.6084/m9.figshare.1164194) (2014).
43. Peixoto, T. P. Hierarchical block structures and high-resolution model selection in large networks. *Phys. Rev. X* **4**, 011047, DOI: [10.1103/PhysRevX.4.011047](https://doi.org/10.1103/PhysRevX.4.011047) (2014).
44. Peixoto, T. P. *Bayesian Stochastic Blockmodeling*, chap. 11, 289–332 (John Wiley & Sons, Ltd, 2019). <https://onlinelibrary.wiley.com/doi/pdf/10.1002/9781119483298.ch11>.
45. Karrer, B. & Newman, M. E. J. Stochastic blockmodels and community structure in networks. *Phys. Rev. E* **83**, 016107, DOI: [10.1103/PhysRevE.83.016107](https://doi.org/10.1103/PhysRevE.83.016107) (2011).
46. Holland, P. W., Laskey, K. B. & Leinhardt, S. Stochastic blockmodels: First steps. *Soc. Networks* **5**, 109–137, DOI: [https://doi.org/10.1016/0378-8733\(83\)90021-7](https://doi.org/10.1016/0378-8733(83)90021-7) (1983).
47. Seguin, C., Mansour L, S., Sporns, O., Zalesky, A. & Calamante, F. Network communication models narrow the gap between the modular organization of structural and functional brain networks. *Neuroimage* **257**, 119323, DOI: [10.1016/j.neuroimage.2022.119323](https://doi.org/10.1016/j.neuroimage.2022.119323) (2022).
48. Song, B. & Avery, L. The pharynx of the nematode *C. elegans*. *Worm* **2**, e21833, DOI: [10.4161/worm.21833](https://doi.org/10.4161/worm.21833) (2013). PMID: 24058858, <https://doi.org/10.4161/worm.21833>.
49. Albertson, D. G. & Thomson, J. N. The pharynx of *Caenorhabditis elegans*. *Philos Trans R Soc Lond B Biol Sci* **275**, 299–325, DOI: [10.1098/rstb.1976.0085](https://doi.org/10.1098/rstb.1976.0085) (1976).

50. Betzel, R., Puxeddu, M. G. & Seguin, C. Hierarchical communities in the larval *Drosophila* connectome: Links to cellular annotations and network topology. *Proc. Natl. Acad. Sci.* **121**, e2320177121, DOI: [10.1073/pnas.2320177121](https://doi.org/10.1073/pnas.2320177121) (2024). <https://www.pnas.org/doi/pdf/10.1073/pnas.2320177121>.
51. Betzel, R., Puxeddu, M. G., Seguin, C. & Misić, B. Parallel and converging multisensory cascades in the *Drosophila* connectome. *bioRxiv* DOI: [10.1101/2024.12.04.624189](https://doi.org/10.1101/2024.12.04.624189) (2024). <https://www.biorxiv.org/content/early/2024/12/08/2024.12.04.624189.full.pdf>.
52. Emmons, S. W. Functions of *C. elegans* neurons from synaptic connectivity. *bioRxiv* DOI: [10.1101/2024.03.08.584145](https://doi.org/10.1101/2024.03.08.584145) (2024).
53. Weinstein, S. M. *et al.* Network enrichment significance testing in brain–phenotype association studies. *Hum. Brain Mapp.* **45**, e26714, DOI: <https://doi.org/10.1002/hbm.26714> (2024). <https://onlinelibrary.wiley.com/doi/pdf/10.1002/hbm.26714>.
54. Li, J. *et al.* Network-level enrichment provides a framework for biological interpretation of machine learning results. *Netw. Neurosci.* **8**, 762–790, DOI: [10.1162/netn\\_a\\_00383](https://doi.org/10.1162/netn_a_00383) (2024). [https://direct.mit.edu/netn/article-pdf/8/3/762/2467417/netn\\_a\\_00383.pdf](https://direct.mit.edu/netn/article-pdf/8/3/762/2467417/netn_a_00383.pdf).
55. Kunin, A. B., Guo, J., Bassler, K. E., Pitkow, X. & Josić, K. Hierarchical modular structure of the *Drosophila* connectome. *J. Neurosci.* **43**, 6384–6400, DOI: [10.1523/JNEUROSCI.0134-23.2023](https://doi.org/10.1523/JNEUROSCI.0134-23.2023) (2023). <https://www.jneurosci.org/content/43/37/6384.full.pdf>.
56. Bargmann, C. I. & Horvitz, H. R. Chemosensory neurons with overlapping functions direct chemotaxis to multiple chemicals in *C. elegans*. *Neuron* **7**, 729–742, DOI: [10.1016/0896-6273\(91\)90276-6](https://doi.org/10.1016/0896-6273(91)90276-6) (1991).
57. Cornelia I Bargmann, I. M. *Chemotaxis and Thermotaxis*. In: *C. elegans II. 2nd edition.*, chap. 25 (Cold Spring Harbor (NY): Cold Spring Harbor Laboratory Press, 1997).
58. Monica Driscoll, J. K. *Mechanotransduction*. In: *C. elegans II. 2nd edition.*, chap. 23 (Cold Spring Harbor (NY): Cold Spring Harbor Laboratory Press, 1997).
59. Kumar, S., Sharma, A. K., Tran, A., Liu, M. & Leifer, A. M. Inhibitory feedback from the motor circuit gates mechanosensory processing in *Caenorhabditis elegans*. *PLoS Biol* **21**, e3002280, DOI: [10.1371/journal.pbio.3002280](https://doi.org/10.1371/journal.pbio.3002280) (2023).

60. Wang, Y. *et al.* Flexible motor sequence generation during stereotyped escape responses. *Elife* **9**, DOI: [10.7554/eLife.56942](https://doi.org/10.7554/eLife.56942) (2020).
61. Kawano, T. *et al.* An imbalancing act: gap junctions reduce the backward motor circuit activity to bias *C. elegans* for forward locomotion. *Neuron* **72**, 572–586, DOI: [10.1016/j.neuron.2011.09.005](https://doi.org/10.1016/j.neuron.2011.09.005) (2011).
62. Gordus, A., Pokala, N., Levy, S., Flavell, S. W. & Bargmann, C. I. Feedback from network states generates variability in a probabilistic olfactory circuit. *Cell* **161**, 215–227, DOI: [10.1016/j.cell.2015.02.018](https://doi.org/10.1016/j.cell.2015.02.018) (2015).
63. Gray, J. M., Hill, J. J. & Bargmann, C. I. A circuit for navigation in *Caenorhabditis elegans*. *Proc Natl Acad Sci U S A* **102**, 3184–3191, DOI: [10.1073/pnas.0409009101](https://doi.org/10.1073/pnas.0409009101) (2005).
64. Chalfie, M. *et al.* The neural circuit for touch sensitivity in *Caenorhabditis elegans*. *J Neurosci* **5**, 956–964, DOI: [10.1523/JNEUROSCI.05-04-00956.1985](https://doi.org/10.1523/JNEUROSCI.05-04-00956.1985) (1985).
65. Tsalik, E. L. & Hobert, O. Functional mapping of neurons that control locomotory behavior in *Caenorhabditis elegans*. *J Neurobiol* **56**, 178–197, DOI: [10.1002/neu.10245](https://doi.org/10.1002/neu.10245) (2003).
66. Meyer, D. L. R. T. B. B. J. & Priess, J. R. (eds.) *C. elegans II. 2nd edition.* (old Spring Harbor (NY): Cold Spring Harbor Laboratory Press, 1997).
67. Betzel, R. F., Medaglia, J. D. & Bassett, D. S. Diversity of meso-scale architecture in human and non-human connectomes. *Nat. Commun.* **9**, 346, DOI: [10.1038/s41467-017-02681-z](https://doi.org/10.1038/s41467-017-02681-z) (2018).
68. Pavlovic, D. M., Vértes, P. E., Bullmore, E. T., Schafer, W. R. & Nichols, T. E. Stochastic block modeling of the modules and core of the *Caenorhabditis elegans* connectome. *PLoS One* **9**, e97584, DOI: [10.1371/journal.pone.0097584](https://doi.org/10.1371/journal.pone.0097584) (2014).
69. Colizza, V., Flammini, A., Serrano, M. A. & Vespignani, A. Detecting rich-club ordering in complex networks. *Nat. Phys.* **2**, 110–115, DOI: [10.1038/nphys209](https://doi.org/10.1038/nphys209) (2006).
70. van den Heuvel, M. P. & Sporns, O. Rich-club organization of the human connectome. *J Neurosci* **31**, 15775–15786, DOI: [10.1523/JNEUROSCI.3539-11.2011](https://doi.org/10.1523/JNEUROSCI.3539-11.2011) (2011).

71. Towilson, E. K., Vértés, P. E., Ahnert, S. E., Schafer, W. R. & Bullmore, E. T. The rich club of the *C. elegans* neuronal connectome. *J Neurosci* **33**, 6380–6387, DOI: [10.1523/JNEUROSCI.3784-12.2013](https://doi.org/10.1523/JNEUROSCI.3784-12.2013) (2013).
72. Rhoades, J. L. *et al.* Asics mediate food responses in an enteric serotonergic neuron that controls foraging behaviors. *Cell* **176**, 85–97.e14, DOI: [10.1016/j.cell.2018.11.023](https://doi.org/10.1016/j.cell.2018.11.023) (2019).
73. Dorkenwald, S. *et al.* Neuronal wiring diagram of an adult brain. *Nature* **634**, 124–138, DOI: [10.1038/s41586-024-07558-y](https://doi.org/10.1038/s41586-024-07558-y) (2024).
74. Lin, A. *et al.* Network statistics of the whole-brain connectome of drosophila. *bioRxiv* DOI: [10.1101/2023.07.29.551086](https://doi.org/10.1101/2023.07.29.551086) (2024).
75. Abbott, L. F. *et al.* The mind of a mouse. *Cell* **182**, 1372–1376, DOI: [10.1016/j.cell.2020.08.010](https://doi.org/10.1016/j.cell.2020.08.010) (2020).
76. Barabási, D. L. *et al.* Neuroscience needs network science. *ArXiv* (2023).
77. Randi, F., Sharma, A., Dvali, S. & Leifer, A. M., DOI: <https://doi.org/10.48324/dandi.001075/0.240920.1434> (2024).
78. Newman, M. E. J. & Girvan, M. Finding and evaluating community structure in networks. *Phys. Rev. E* **69**, 026113, DOI: [10.1103/PhysRevE.69.026113](https://doi.org/10.1103/PhysRevE.69.026113) (2004).
79. Rosvall, M. & Bergstrom, C. T. Maps of random walks on complex networks reveal community structure. *Proc. Natl. Acad. Sci.* **105**, 1118–1123, DOI: [10.1073/pnas.0706851105](https://doi.org/10.1073/pnas.0706851105) (2008). <https://www.pnas.org/doi/pdf/10.1073/pnas.0706851105>.

## Acknowledgments

Research reported in this work was supported by the National Institutes of Health National Institute of Neurological Disorders and Stroke under New Innovator award number DP2-NS116768 to A.M.L.; the Simons Foundation under award SCGB #543003 to A.M.L.; by the National Science Foundation, through the Center for the Physics of Biological Function (PHY-1734030); by the National Science Foundation under award number 2023985 to R.F.B.; by the National Institute of Aging (5R01AG075044-03) to R.F.B.;

by the National Institute on Drug Abuse (1RF1NS125026-01A1) to R.F.B; by the Boehringer Ingelheim Fonds to S.D.;

## **Author contributions**

Conceptualization: S.D., C.S., R.B. and A.M.L.; Formal analysis: S.D.; Funding acquisition: A.M.L.; Investigation: S.D.; Methodology: S.D., C.S. and R.B.; Project administration: A.M.L.; Supervision: A.M.L.; Visualization: S.D.; Writing – original draft: S.D.; Writing - review & editing: S.D., C.S., R.B. and A.M.L.;

## **Competing Interests**

There are no competing interests.

## **Additional Information**

To whom correspondence should be addressed: leifer@princeton.edu

## **Code availability**

Code available at <https://github.com/SophieDvali/FunconnNetworkAnalysis>

## Methods

**The Networks** The *C. elegans* connectome we use consists of electrical and chemical synapses between pairs of neurons from three adults and one L4 EM datasets [23, 25]. We binarize the connectome in the following way: Two neurons in the anatomical network are considered connected if there is at least one connection between them in any of the four connectome datasets. The signal propagation network was experimentally measured via direct optogenetic activation and simultaneous whole-brain calcium imaging [14]. The signal propagation dataset can be found at <https://dandiarchive.org/dandiset/001075/0.240920.1434>[77]. Neurons are considered to be statistically significantly functionally connected if they have a q-value of less than 0.05. Both networks contain the 188 head neurons of the 302 total *C. elegans* neurons.

**Stochastic Block Modeling** Hierarchical community assignments were determined by finding the best partition using the graph-tool python module agglomerative multilevel Markov chain Monte Carlo (MCMC) algorithm in a degree-corrected manner [42][43][44] (<https://graph-tool.skewed.de/static/doc/demos/inference/inference.html>). Here, the inferred "best" partition of the communities comes from sampling the equilibrated Markov chain many times, aligning communities, and for each neuron taking the mode of its assignment. Neither networks were weighted.

**Bilaterally symmetric neurons** The probability of two bilaterally symmetric neurons being in the same community and not in the same community were calculated by dividing the number of pairs in the same community and not in the same community respectively by the total number of bilateral pairs. The p-value was determined by comparing the probabilities to a null distribution of probabilities derived from shuffled community assignments via a one-sided t-test.

**Enrichment Analysis** Community enrichment was determined by calculating the overlap of the set of neurons with a given cell annotation and the set of neurons in a given community (or in the case of comparing the communities of both networks the overlap of the set of neurons in each of the network communities). We then also calculate a null distribution of overlaps for 1000 shuffled community assignments. We then compare the original overlap to the null distribution to determine a z-score and

p-value (one-sided t-test) for enrichment. P-values are adjusted for multiple hypotheses using FDR.

**Module-matching** For each pair of communities (anatomical and signal propagation), we calculate the Jaccard score to obtain a similarity matrix. The similarity matrix is then reorganized via the Hungarian method to determine the anatomical communities that best correspond to each of the signal propagation communities.

**Community Motifs Analysis** Unlike some common methods for community detection designed to detect “assortative” community structure—e.g. modularity maximization [78] or infomap [79]—the stochastic blockmodel can detect generic types of community structure. These include core-periphery and disassortative motifs. To determine if the detected communities in the signaling network exhibited these types of non-assortative interactions (as well as the more common assortative type), we followed a recently-proposed method [67]. Specifically, we considered community pairs and their within- and between-community densities of connections. Specifically, for communities  $r$  and  $s$ , we consider the within-community densities,  $\omega_{rr}$  and  $\omega_{ss}$ , as well as the between-community density,  $\omega_{rs}$ . Given these values, we unambiguously classified the interaction between  $r$  and  $s$  as assortative if  $\omega_{rr} > \omega_{rs}$  and  $\omega_{ss} > \omega_{rs}$ . Conversely, the interaction was *disassortative* if  $\omega_{rs} > \omega_{rr}$  and  $\omega_{rs} > \omega_{ss}$ . The core-periphery motif corresponded to the case where  $\omega_{rr} > \omega_{rs} > \omega_{ss}$ . In this case, communities  $r$  and  $s$  were labeled as the core and the periphery, respectively (note that  $\omega_{ss} > \omega_{rs} > \omega_{rr}$  would also be considered a core-periphery motif, but with the roles reversed).

After classifying a community motif, we then passed the classification labels back to the nodes (neurons) that made up community  $r$  and community  $s$ . That is, if the interaction between  $r$  and  $s$  was labeled “assortative”, then all the neurons in  $r$  and all the neurons in  $s$  were assigned an assortative label. We repeated the assignment for all pairs of communities and calculated how frequently neurons were assigned one of the four classes (assortative, disassortative, core, and periphery).

**Determining the Rich Club** To determine whether the signaling network contains a rich club we calculate the rich club coefficient  $\Phi(k)$  across for every degree  $k$ . The rich club coefficient measures the density of connections among nodes with degree greater than  $k$ . We then compare  $\Phi(k)$  for our network to the average  $\Phi(k)_{rand}$  calculated across 1000 random networks. While  $\Phi(k)$  was determined to be

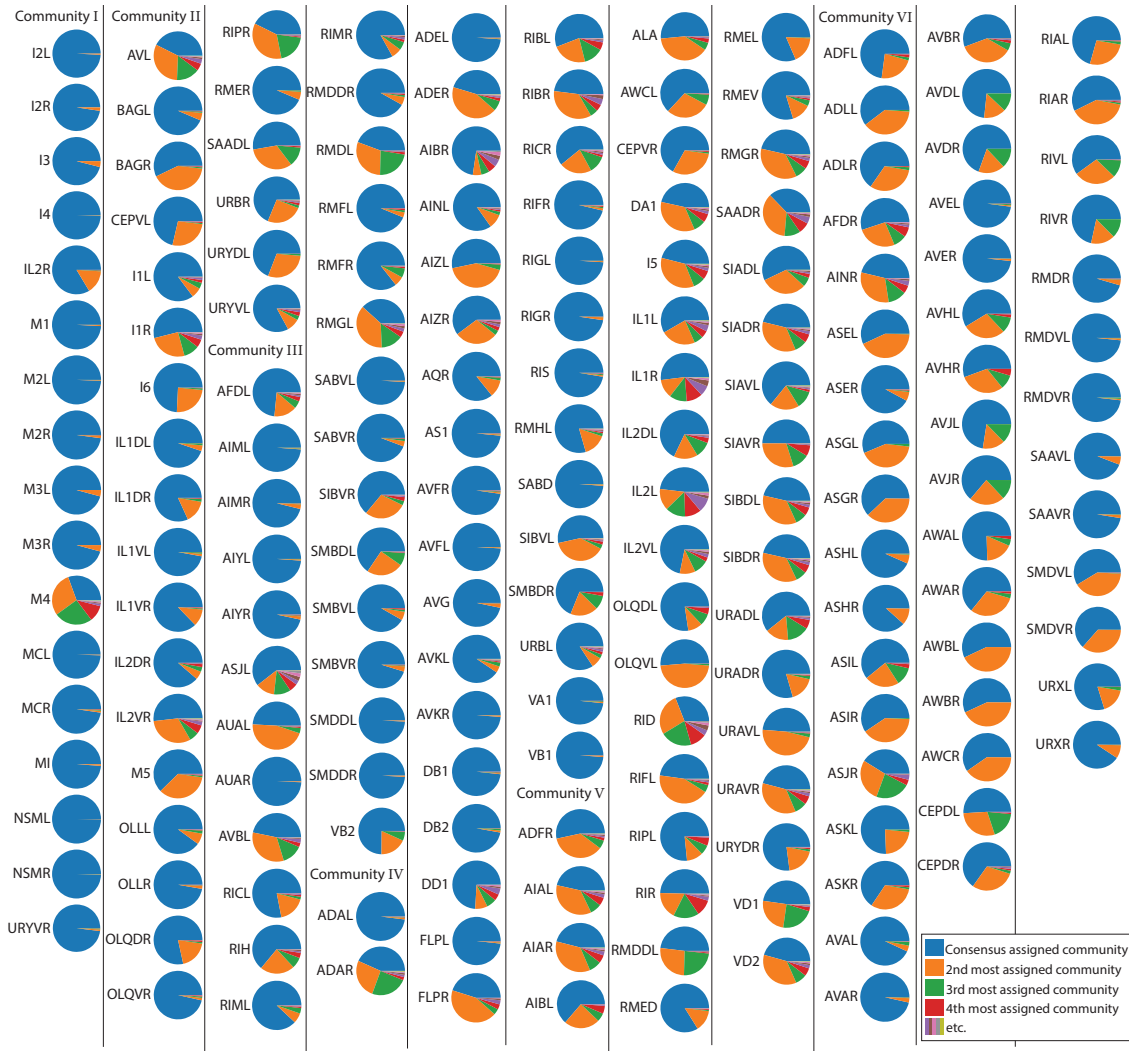


statistically significantly larger than  $\langle \Phi(k)_{rand} \rangle$  from  $k = 3$  onwards we concentrated on the two local maxima in  $\Phi(k)_{norm}$  at  $k = 25$  and  $k = 40$ .

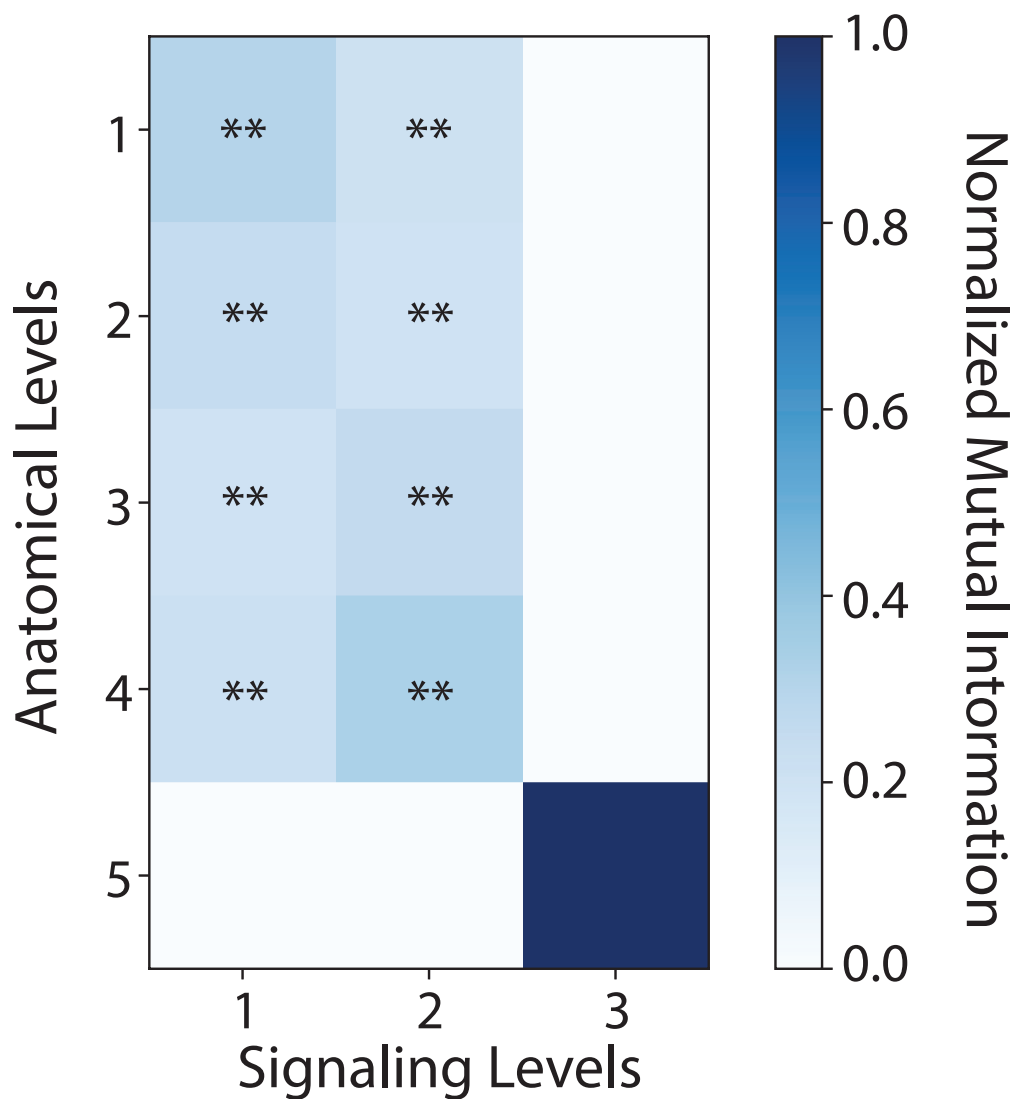
## Extended Data

Triad type	Nr. of Structures			
	Signaling Network	Erdos-renyi signaling density	Anatomical Network	Erdos-renyi anatomical density
	3047	3067.8	5606	19144.4
	2667	3054.2	7195	19317.6
	4007	6127.8	6751	38589.2
	503	205	1697	3973.4
	1629	203.2	10231	3672
	1373	203	11056	3681
	158	4	1485	179.4
	157	3	1388	193.6
	147	6.6	596	373
	226	4.4	6239	177.8
	172	0	2020	36.6
	172	0	826	0.2
	60	71	48	1314

**Extended Data Figure 1. The distribution of triad structures.** Occurrences of the 13 possible triad structures in the signaling and anatomical networks compared to the average from five random Erdos-renyi graphs with the same number of nodes and density as the signaling network (third column) and the anatomical network (fifth column)



**Extended Data Figure 2. Variability in community assignment by neuron.** Pie charts indicate how consistently neurons were assigned to the same community in the structural network. Organized by community. Blue corresponds to the fraction assigned to the consensus community assignment (largest fraction), orange the next most common community assignment then green etc.



**Extended Data Figure 3. Comparison of signaling and anatomical communities.** Normalized mutual information between the community assignment of neurons pairwise between hierarchical levels in the anatomical and signaling communities. \*\* indicates a FDR adjusted  $p > 0.05$  compared to randomly shuffled community assignments. The last community of both the anatomical and signaling networks only has one community that includes all of the neurons.

**a**

**Sensory:** ADEL, ADER, ADFL, ADFR, ADLL, ADLR, AFDL, AFDR, AQR, ASEL, ASER, ASGL, ASGR, ASHL, ASHR, ASIL, ASIR, ASJL, ASJR, ASKL, ASKR, AUAL, AUAR, AVG, AWAL, AWAR, AWBL, AWBR, AWCL, AWCR, BAGL, BAGR, CEPDL, CEPDR, CEPVL, CEPVR, FLPL, FLPR, IL1DL, IL1DR, IL1L, IL1R, IL1VL, IL1VR, IL2DL, IL2DR, IL2L, IL2R, IL2VL, IL2VR, NSML, NSMR, OLLL, OLLR, OLQDL, OLQDR, OLQVL, OLQVR, URADL, URADR, URAVL, URAVR, URBL, URBR, URXL, URXR, URYDL, URYDR, URYVL, URYVR

**Inter:** ADAL, ADAR, AIAL, AIAR, AIBL, AIBR, AIML, AIMR, AINL, AINR, AIYL, AIYR, AIZL, AIZR, ALA, AVAL, AVAR, AVBL, AVBR, AVDL, AVDR, AVEL, AVER, AVFL, AVFR, AVHL, AVHR, AVJL, AVJR, AVKL, AVKR, AVL, I1L, I1R, I2L, I2R, I3, I4, I5, I6, RIAL, RIAR, RIBL, RIBR, RICL, RICR, RIFL, RIFR, RIGL, RIGR, RIH, RIPL, RIPR, RIR, RIS, RIVL, RIVR, SAADL, SAADR, SAAVL, SAAVR, SABD, SABV, SABVR, SIADL, SIADR, SIAVL, SIAVR, SIBDL, SIBDR, SIBVL, SIBVR

**Motor:** AS1, DA1, DB1, DB2, DD1, M1, M2L, M2R, M3L, M3R, M4, M5, MCL, MCR, MI, RID, RIML, RIMR, RMDDL, RMDDR, RMDL, RMDR, RMDVL, RMDVR, RMED, RMEL, RMER, RMEV, RMFL, RMFR, RMGL, RMGR, RMHL, SMBDL, SMBDR, SMBVL, SMBVR, SMDDL, SMDDR, SMDVL, SMDVR, VA1, VB1, VB2, VD1, VD2

**b**

**Pharynx:** I1L, I1R, I2L, I2R, I3, I4, I5, I6, M1, M2L, M2R, M3L, M3R, M4, M5, MCL, MCR, MI, NSML, NSMR

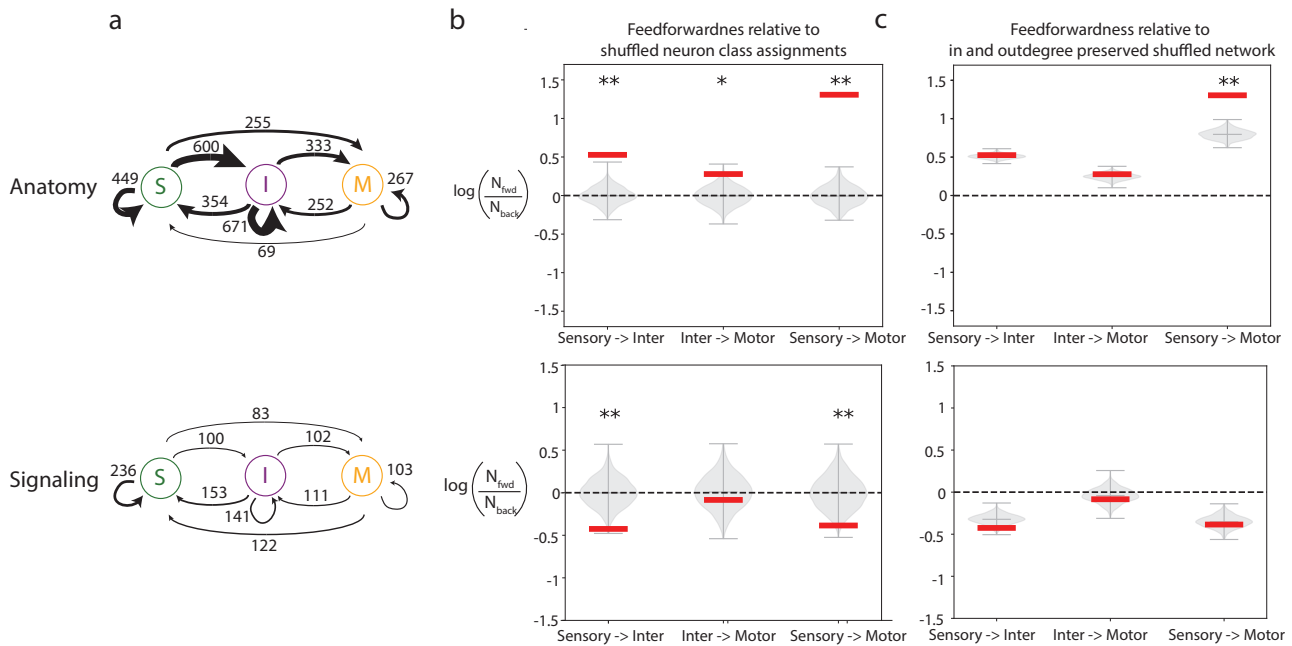
**VNC motor:** DA1, DB1, DB2, AS1, DD1, VA1, VB1, VB2, VD1, VD2

**Amphid sensory:** ADFL, ADLL, AFDL, ASEL, ASGL, ASHL, ASIL, ASJL, ASKL, AWAL, AWBL, AWCL, ADFR, ADLR, AFDR, ASER, ASGR, ASHR, ASIR, ASJR, ASKR, AWAR, AWBR, AWCR

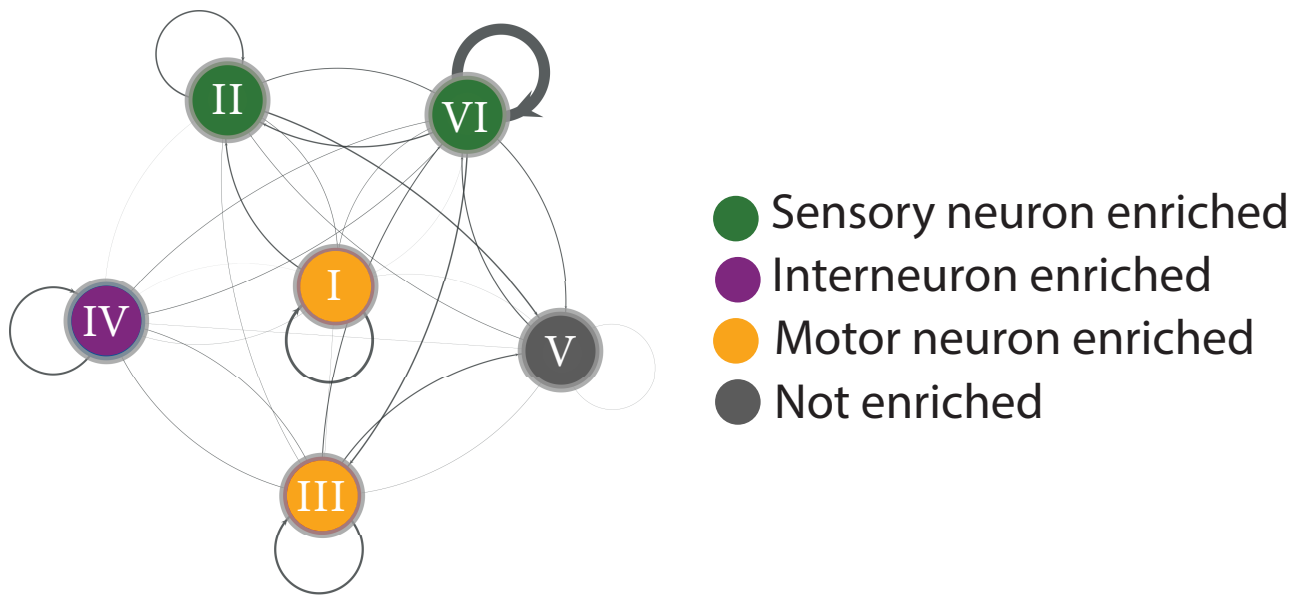
**Locomortory inter:** AVAL, AVAR, AVBL, AVBR, AVDL, AVDR, AVEL, AVER

**Ring inter:** ADAL, ADAR, AIML, AIMR, AINL, AINR, RIAL, RIAR, RIBL, RIBR, RICL, RICR, RID, RIFL, RIFR, RIGL, RIGR, RIH, RIPL, RIPR, RIR, RIS, RIVL, RIVR, SAADL, SAADR, SAAVL, SAAVR, SABD, SABVL, SABVR

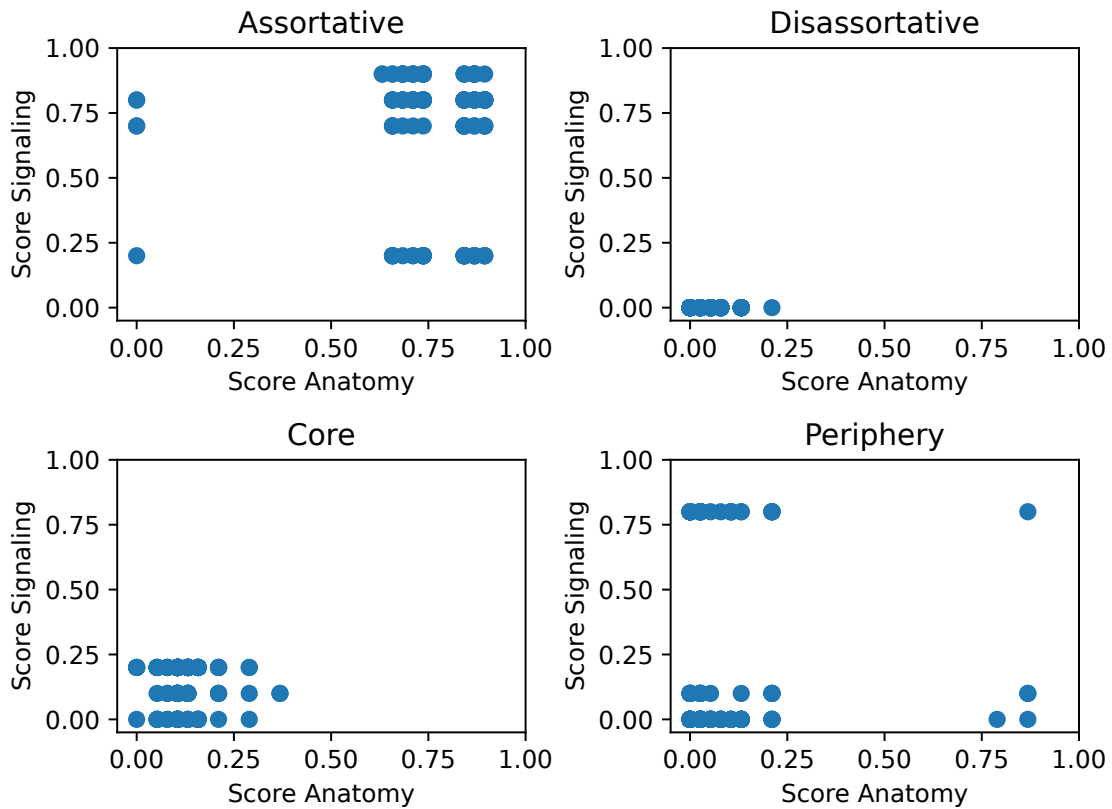
**Extended Data Figure 4. Neuron type and role annotations. a)** Neurons in the different neuron types (sensory, inter- and motor neurons) **b)** Neurons with different roles



**Extended Data Figure 5. Anatomy is net feed-forward along the sensory to inter- to motor neuron pathway while signaling is ambiguous.** **a)** Number of edges between sensory, inter-, and motor neurons for anatomy (top) and signaling (top). Arrow thickness is proportional to the number of edges along the arrow. **b)** log of the ratio of the number of edges forwards to backwards along the sensory  $\rightarrow$  inter  $\rightarrow$  motor pathway for each possible leg of the pathway: sensory  $\rightarrow$  interneurons, inter-  $\rightarrow$  motor neurons and sensory  $\rightarrow$  motor neurons. Anything above 0 indicates more forwards than backward edges implying feed-forwardness, anything below indicates more backward than forward edges implying feed-backwardness. Red indicates the true log of the ratio of the number of edges. Grey violin plots are derived from a control in which assignments of the labels "sensory", "inter" and "motor" are shuffled. **c)** Same as b) except the grey violin plots are derived instead from a control where the network is shuffled in a way that preserves the total in and out-degree of each neuron. (\*  $p < 0.05$ , \*\*  $p < 0.01$ , p-values calculated via a two-sided t-test)

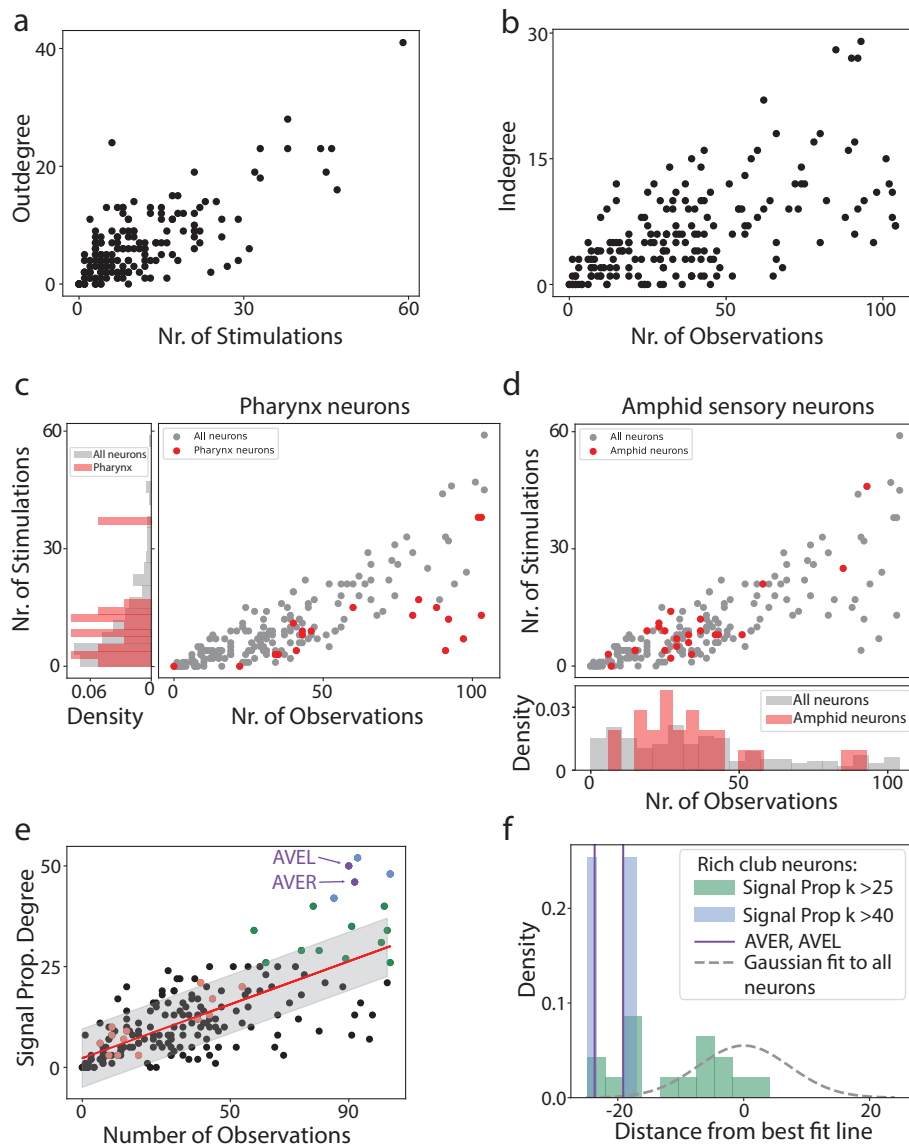


**Extended Data Figure 6. Network diagram of edges between the six communities.** Communities are colored by whether they are enriched for sensory (green), inter- (purple), motor neurons (yellow), or not enriched for any neuron type (grey). Arrow thickness indicates the fraction of all possible edges between nodes in the source community and the target community



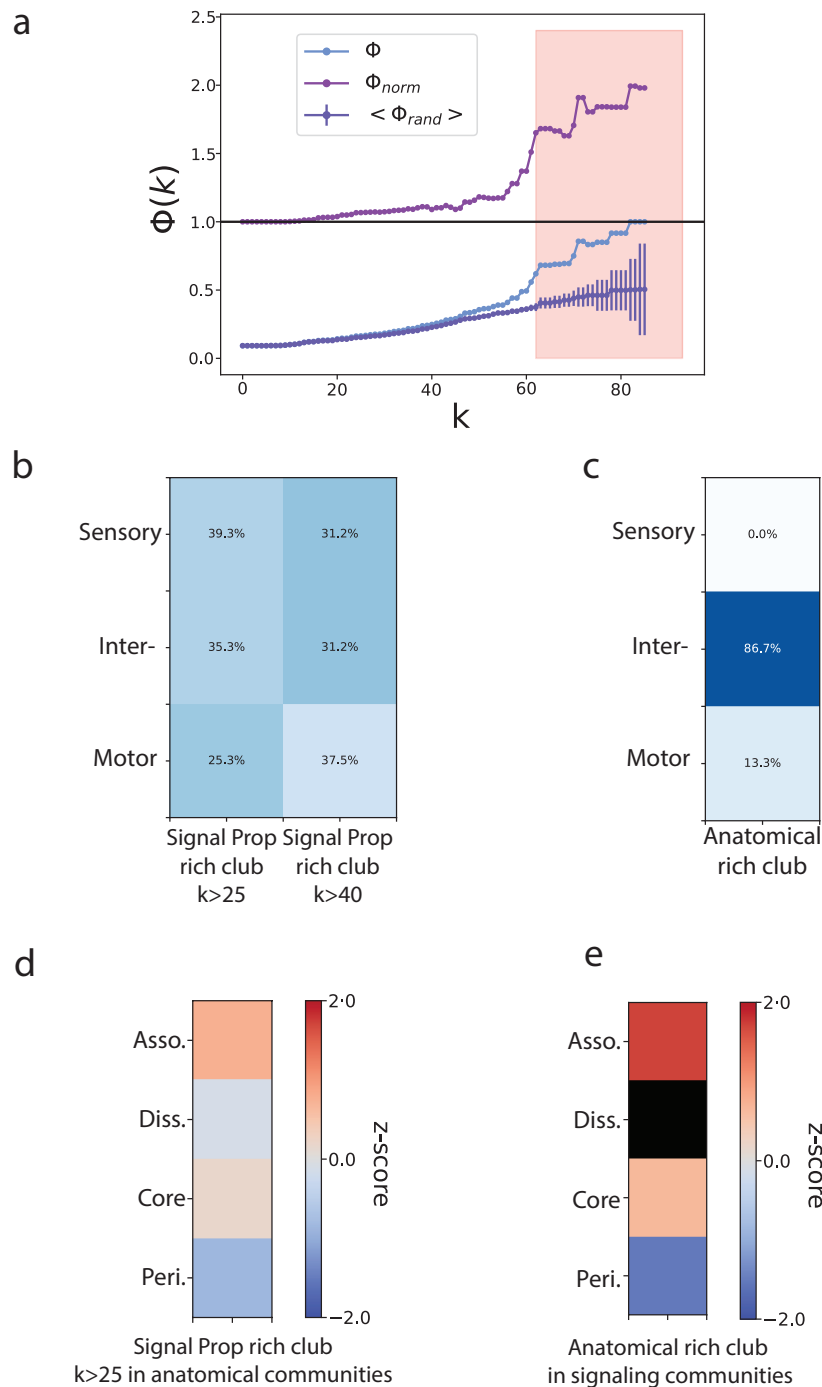
**Extended Data Figure 7. Comparison of community motif score in anatomy and signaling.** Score assigned to each neuron for participating in assortative, disassortative, core, and periphery interactions in the anatomical network vs the signaling network





**Extended Data Figure 8. Broadcaster, integrator and rich club results are not a trivial**

**consequence of the number of stimulations and observations of neurons.** **a)** Scatter plot of out-degree and number of stimulations of all neurons. **b)** Scatter plot of the in-degree and the number of observations of all neurons **c)** Right panel: Histogram of the density of the number of stimulations of all neurons (grey) and pharynx neurons (red). Left panel: Scatter plot of the number of observations and the number of stimulations of all neurons (grey) and pharynx neurons (red). Pharynx neurons do not have a larger than expected number of stimulations compared to all other neurons (Kolmogorov-Smirnoff test  $p$ -value = 0.9) **d)** Upper panel: Scatter plot of the number of observations and the number of stimulations of all neurons (grey) and amphid sensory neurons (red). Lower panel: Histogram of the density of the number of observations of all neurons (grey) and amphid neurons (red). Amphid neurons do not have a larger than expected number of observations compared to all other neurons (Kolmogorov-Smirnoff test  $p$ -value = 0.38) **e)** Correlation between the number of observations and signal propagation degree (pearsons correlation  $r = 0.71$ ). Green: signaling rich club neurons of  $k > 25$ , blue: signaling rich club of neurons  $k > 40$ , red: anatomical rich club neuron, purple: neurons in both signaling and anatomical rich clubs. **f)** Histogram of neurons distance from the best-fit line in e). Dashed grey line shows the Gaussian fit to the histogram of all neurons. Blue and green show the histograms of the signaling rich club neurons with  $k > 40$  and  $k > 25$  respectively. Purple bars show neurons AVEL/R.



**Extended Data Figure 9. Rich Club.** **a)** The anatomical network has a rich club. Light blue: rich club coefficient of the anatomical connectome, dark blue: average rich club coefficient of 100 randomized anatomical networks (edges rewired randomly but the degree sequence remains the same) error bars represent standard deviation, purple: normalized rich club coefficient. **b)** Sensory, inter-, and motor neuron makeup of the signal propagation rich club. **c)** Sensory, inter-, and motor neuron makeup of the anatomical rich club. **d)** Enrichment (z-score) of neurons belonging to the signaling rich club for assortative, disassortative, and core/periphery interactions in the anatomical network (\*  $p < 0.05$ , \*\*  $p < 0.01$ , p-values FDR-adjusted). **e)** Enrichment (z-score) of neurons belonging to the anatomical rich club for assortative, disassortative, and core/periphery interactions in the signaling network (\*  $p < 0.05$ , \*\*  $p < 0.01$ , p-values FDR-adjusted)